# Chapter 8
# The Hydrological Cycle of the Mediterranean

**Pinhas Alpert, Debbie Hemmings, Fengjun Jin, Gillian Kay, Akio Kitoh, and Annarita Mariotti**



**Abstract** The water cycle components over the Mediterranean both for current and future run are studied with the ensemble of CMIP3 multi-model simulations and with the Japan Meteorological Agency's 20 km grid global climate model. Results from the JMA model are compared to the CMIP3 ensemble model (here after Mariotti). CMIP3 results are surprisingly close to JMAs. The projected mean annual change rate of precipitation (P) between future and current run for sea and land, are −11% and −10%, respectively in the JMA run, not as high as Mariotti's. Projected changes for evaporation (E) are +9.3% and −3.6%, compared to +7.2% and −8.1% in Mariotti's study. However, no significant difference of change in P–E over the sea body is found between these two studies. The increased E over the eastern Mediterranean was found higher than the western Mediterranean, but the P decrease is lower. The net moisture budget, P-E, shows that the eastern Mediterranean will become even drier than the western Mediterranean. The river model suggests significant decreases in water inflow to the Mediterranean of about 36% in the JMA run (excluding the Nile). The Palmer Drought Severity Index (PDSI), which reflects the combined effects of precipitation and surface air temperature (Ts) changes,

P. Alpert (✉) • F. Jin
[AU1] Tel-Aviv University, TAU, Tel-Aviv, Israel
e-mail: pinhas@cyclone.tau.ac.il

D. Hemmings • G. Kay
Met Office, Hadley Centre, Exeter, Devon, UK

A. Kitoh
JAMSTEC/MRI, Tsukuba, Japan

A. Mariotti
Italian National Agency for New Technologies, Energy and Sustainable Economic Development, Rome, Italy

Earth System Science Interdisciplinary Center, University of Maryland, College Park, MD, USA

A. Navarra and L. Tubiana (eds.), *Regional Assessment of Climate Change in the Mediterranean*, Advances in Global Change Research 50,
DOI 10.1007/978-94-007-5781-3_8, 

shows a progressive and substantial drying of Mediterranean land surface over this region since 1900 (−0.2 PDSI units/decade) consistent with a decrease in precipitation and an increase in surface temperature, Ts (not shown). The last chapter reports on five climate model projections of changes in aspects of the hydrological cycle for the Mediterranean region. Three of these models have an interactive Mediterranean Sea, and two are versions of the Met Office Hadley Centre regional model with different land surface schemes. The focus is upon changes in evapotranspiration, and how these changes could be important in controlling available renewable water resources (runoff). Rainfall is projected to decline across large areas by over 20% in all of the models, although in the Météo-France model, the central part of the northern Mediterranean domain, such as over southern Italy and Greece, has areas of increase as well as decrease. In pockets of Turkey, the eastern Mediterranean, Italy and Spain, projections from the MPI, HadRM3-MOSES2, HadRM3-MOSES1 and ENEA models are for decreases in summer rainfall of 50% or more. Consistent with the global model projections, each of the five high-resolution models simulate higher temperatures and reduced evapotranspiration and precipitation for much of the Mediterranean region by the middle of this century. The strongest and most widespread reductions in precipitation projected to occur in the spring and summer seasons, while reductions in evapotranspiration are most severe in summer.

**Keywords** Mediterranean • Water cycle • Super- High-Resolution Climate Model • Rivers • Global Warming • Evapotranspiration • Water budget

## 8.1 Long-Term Changes in Mediterranean Sea Water Cycle: Observed and Projected

### *8.1.1 Introduction*

In view of the semi-enclosed nature of the Mediterranean/Black Sea system, connected to the Atlantic Ocean via the Strait of Gibraltar, and the semi-arid/arid conditions in land regions downstream of Mediterranean moisture fluxes, the impacts of changes in the Mediterranean Sea water cycle may be substantial. For example, increases in sea evaporation (the biggest single component of Mediterranean water cycle) and fresh water loss affect the salt, water and energy budgets with potentially important implications for Mediterranean Sea salinity (note that Mediterranean Sea salinity is among the highest globally), circulation and sea-level (e.g. Skliris et al. 2007; Tsimplis et al. 2008) and Atlantic circulation via changes in Gibraltar water fluxes (Lozier and Stewart 2008; Millot et al. 2006; Potter and Lozier 2004; Reid 1979). Additionally, an increase in evaporation (i.e. due to the amount of moisture the Mediterranean Sea injected into the overlying atmosphere) can enhance moisture fluxes to downstream regions, potentially affecting precipitation there (e.g. in the Sahel Jung et al. (2006)).

In spite of their importance, changes in sea evaporation and sea-surface fresh water fluxes (potentially a combination of precipitation and evaporation changes) in recent past, are yet to be quantified. A number of previous studies have indicated a long-term increase in Western Mediterranean Deep Water salinity and temperatures during the latter half of the twentieth century (e.g. Bethoux et al. 1998; Krahmann 1998; Rixen et al. 2005). Several of these studies have evidenced the linkage between this salinity increase and the long-term decrease in Mediterranean precipitation during the period mid-1970s to early-1990s, primarily in connection with the decadal variations of the North Atlantic Oscillation (Hurrell 1995; Mariotti et al. 2002). Long-term salinity increase has also been connected to a reduction in river discharge (e.g. damming of the Nile River in the 1960s) and Black Sea fresh water inputs (Rohling and Bryden 1992; Skliris et al. 2007). Interannual evaporation anomalies and associated cooling have been identified as a key factor in the Eastern Mediterranean Transient event of 1991–1993 (Josey 2003; Roether et al. 2007). However, decadal evaporation changes over the Mediterranean Sea are still virtually unknown, as previous attempts were limited by data availability (e.g. Krahmann 1998; Mariotti et al. 2002). In fact, both oceanic precipitation and evaporation estimates and their interdecadal variability have remained long elusive in the absence of suitable climatic datasets. Substantial data developments in the last decade, with some datasets now going back 25 years or more, have brought major new opportunities to investigate long-term water cycle variability in oceanic regions (e.g. Adler et al. 2003; Wentz et al. 2007; Yu 2007; Yu and Weller 2007).

A better picture and understanding of recent past long-term water cycle changes in the Mediterranean region is urgently needed as projections of future global climate change indicate major changes for this region in particular as a "Hot Spot" in hydrological change (IPCC 2007a). A number of investigations indicate significant impacts on both mean precipitation and variability (Gibelin and Deque 2003; Giorgi 2006; Giorgi and Lionello 2008; Sheffield and Wood 2008; Ulbrich et al. 2006). However, the combined effects of future precipitation decrease and increasing surface temperature on Mediterranean water cycle, and in particular the impact on Mediterranean Sea water budget, are less well known. Here we present results from a couple recent studies investigating future changes in Mediterranean Sea water cycle, and observed past recent long-term changes performed in the framework of CIRCE (Mariotti et al. 2008; Mariotti 2010). In the first of these studies, the World Climate Research Program Coupled Model Intercomparison Project Phase 3 (CMIP3 hereafter) multi-model projections are used to show how individual hydro-climatic changes will concur to determine even greater alterations of future Mediterranean water cycle characteristics, with contrasting behavior over land and the Mediterranean Sea. Results focus on the "transition phase" from recent past conditions to the much drier conditions expected at the end of the twenty-first century. Finally, an observational analysis explores regional long-term global water cycle changes exploiting recent progress in data availability (Mariotti 2010). The focus is on the combined effects of precipitation and evaporation changes on Mediterranean water cycle. A major question which this investigation addresses is whether the behavior observed during the last few decades is consistent with the

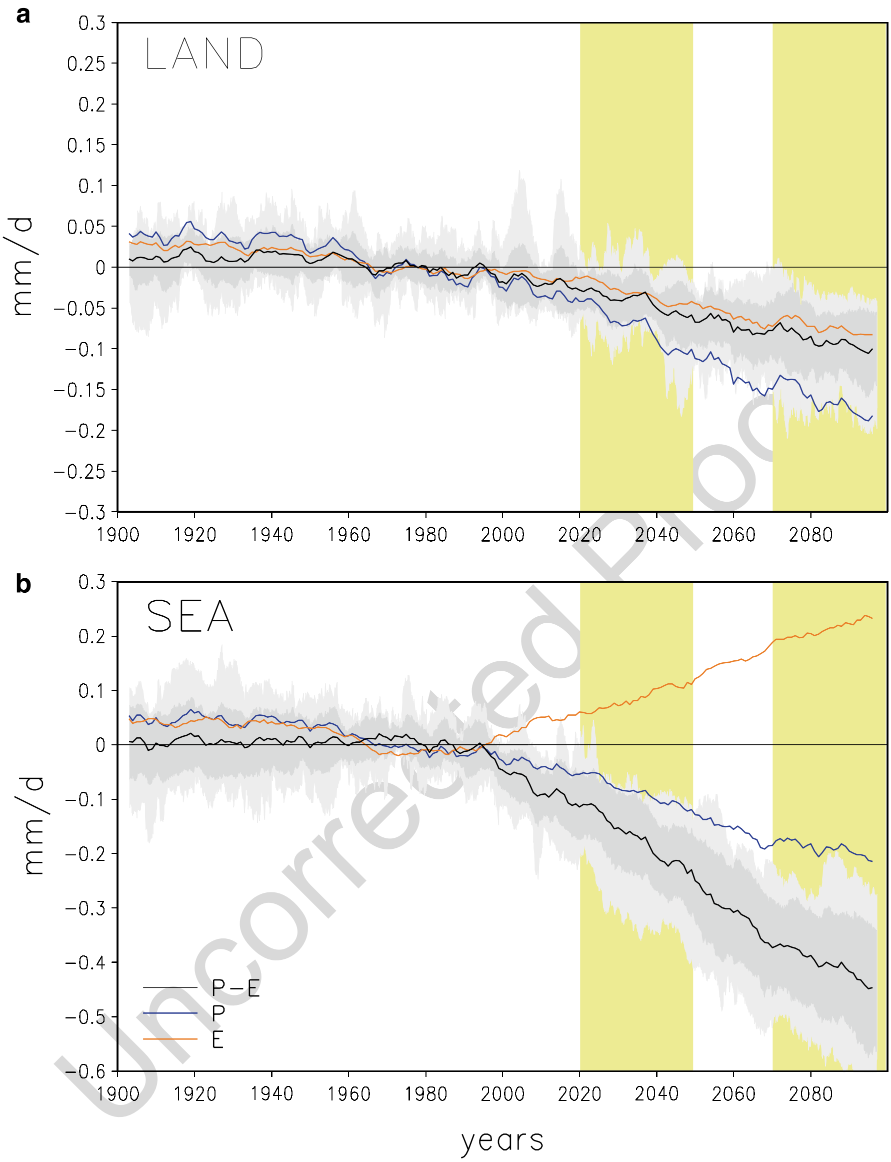




**Fig. 8.1** Mediterranean water cycle anomalies over the period 1900–2100 relative to 1950–2000. Area-averaged evaporation (*brown*), precipitation (*blue*) and precipitation minus evaporation (*black*; P-E) are based on an average of CMIP3 model runs. For P-E, the envelope of individual model anomalies and the 1 standard deviation interval around the ensemble mean are also shown (*light grey* and *dark grey* shading respectively). Data are 6-years running means of annual mean area-averages over the box of Fig. 8.3 broadly defining the Mediterranean region. (Panel **a**) Land-only. (Panel **b**) Sea-only. Focus periods are highlighted (*yellow*) (From Mariotti et al. (2008))

[AU2]

**Table 8.1** Mediterranean averaged precipitation (*P*), evaporation (*E*) and precipitation minus evaporation (*P–E*) anomalies in 2070–2099 relative to 1950–2000

| | P | E | P–E |
|---|---|---|---|
| **(a)** | *Land* | | |
| Annual | −15.5%/−0.17 | −8.1%/−0.08 | −0.09 |
| Wet | −9.7%/−0.12 | −1.5%/−0.01 | −19.6%/−0.11 |
| Dry | −23.6%/−0.21 | −11.8%/−0.14 | −23.4%/−0.07 |
| **(b)** | *Sea* | | |
| Annual | −15.0%/−0.19 | 7.2%/0.21 | −24.2%/−0.41 |
| Wet | −11.6%/−0.22 | 7.5%/0.26 | −29.6%/−0.48 |
| Dry | −23.8%/−0.17 | 6.7%/0.17 | −19.2%/−0.34 |

(Part a) Land-only. (Part b) Sea-only. In each column: annual, “wet” and “dry” mean anomalies based on an average of CMIP3 model runs; relative (%; left) and absolute (mm/day; right) values are reported (annual P-E anomaly over land is absolute value only) (From Mariotti et al. (2008))

“transition” phase suggested by the CMIP3 simulations for the Mediterranean as a pathway toward future projected changes. An overview of key results from these studies is offered here; the reader is referred to the original publications for further information regarding data and methodologies.



### *8.1.2 Simulated and Projected Mediterranean Water Cycle Changes*

An ensemble of CMIP3 multi-model simulations shows a progressive decrease in rainfall in the Mediterranean region that has been on-going during the twentieth century (–0.007 mm/d per decade) and accelerates around the turn of the twenty-first century, followed by rapid drying from 2020 and onwards (Fig. 8.1; –0.02 mm/d per decade).

Projected changes would cause Mediterranean land regions to become gradually more arid, with roughly 15% less precipitation in 2070–2099 compared to 1950–2000, and an 8% decrease already by 2020–2049 (see Table 8.1).

The amplitude of the mean change foreseen by 2020–2049 (about 0.1 mm/d) is comparable to that of the driest spells experienced by the region during the twentieth century (see Figs. 8.1 and 8.4). Since the multi-model ensemble average has internal variability with reduced amplitude, the actual variability, with multi-year droughts and pluvials, would cause greater changes than those depicted by the ensemble mean. As precipitation is the main driver of land surface hydrological cycle, other major hydrological indicators would also change correspondingly. Soil moisture progressively decreases (similar results were found by Gibelin and Deque (2003); so would runoff and river discharge, reducing the water available for irrigation and other uses. Because of the drier land surface, evapotranspiration (evaporation hereafter) would also decrease but, as increased surface temperature favors higher evaporation, the rate would be half that of precipitation. By 2070–2099, effective precipitation (P-E) decrease over land is about −0.09 mm/d (−0.01 mm/d per decade).

While the drying on land is large, the projection over the Mediterranean Sea is even more dramatic. Unlike the surrounding land region where evaporation decreases, the precipitation reduction over the Sea is accompanied by a roughly equal increase in evaporation due to increased sea surface temperature (ultimately due to more energy input from greenhouse warming). As a result, a 24% (0.4 mm/d) increase in the loss of freshwater (E–P) at the sea surface is projected towards the end of the twenty-first century. This change is large, roughly equal to what is typically received in total by the Mediterranean Sea on an annual basis as discharge from neighboring land and as inflow from the Black Sea (Mariotti et al. 2002). Currently a main freshwater source to the southeastern Mediterranean, the Black Sea inflow may also change as it will receive less fresh water at the surface. As a result, the freshwater deficit which already characterizes the Mediterranean Sea would significantly increase, with a cumulative freshwater deficit by 2100 of $1.54 \times 10^8$ m$^3$ (trend is −0.045 mm/d per decade). This would be further exacerbated by the decrease in river discharge from surrounding regions (cumulative decrease is $2.54 \times 10^7$ m$^3$). As in the past, this can have important implications for the Mediterranean Sea (Rohling and Hilgen 1991). Overall, the increase in the Sea's freshwater deficit would contribute to increase salinity. The degree of the salinity increase would depend on the strength of the fresh water input from the Atlantic Ocean at the Gibraltar Strait. [AU3]

Climate change projections typically suffer from major uncertainties with models often not even agreeing on the direction of change (IPCC 2007a), but model consistency regarding twenty-first century Mediterranean water cycle change is among the highest. Most models show a decrease in P-E already by 2020–2049, all by 2070–2099 (Fig. 8.1). By 2070–2099, all models show a decrease in precipitation and an increase in evaporation over the Sea; most show a more moderate decrease in evaporation on land. Fresh water deficit increase over the Sea is estimated between −0.25 and −0.55 mm/d. A recent study in the framework of the ENSEMBLES project based on regional climate model projections also finds broadly similar results (Sanchez-Gomez et al. 2009).

In CMIP3 simulations, precipitation is projected to decrease throughout the year and particularly during the dry season (Fig. 8.2; about −10 and −23% for the wet and dry seasons, respectively; see Table 8.1).

In contrast, most of the land evaporation decrease occurs during the summer dry season (−12%) when land-surface aridity will be greatest. The combination of these changes results in a decrease in effective precipitation that is similar during the wet and dry seasons (about 20%). Over the Sea, freshwater deficit would increase throughout the year and particularly during the wet season when evaporation increase is at a maximum (about 7%).

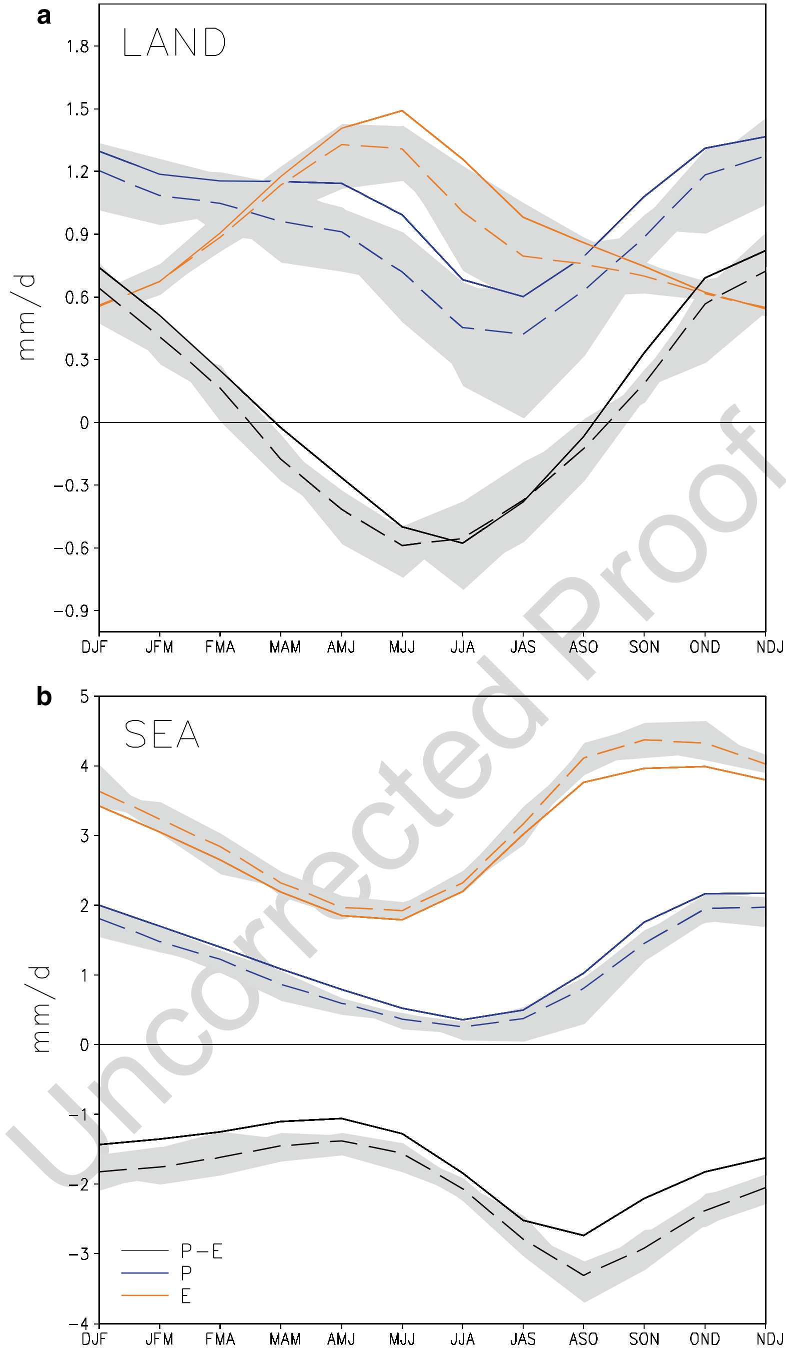




**Fig. 8.2** Mediterranean water cycle in 2070–2099 (*dashed*) compared to the 1950–2000 period (*solid*) based on an average of CMIP3 model simulations. Shown are the seasonal cycles of evaporation (*brown*), precipitation (*blue*) and precipitation minus evaporation (*black*). For each, *grey* shading depicts the envelope of individual model anomalies. (**a**) Land-only (**b**) Sea-only (From Mariotti et al. (2008))

**Table 8.2** Long-term trends in Mediterranean-averaged land-precipitation (P) and precipitation minus evaporation (P–E) for the periods 1900–2007, 2000–2050 and 2000–2099

| | 1900–2007 | 2000–2050 | 2000–2099 |
|---|---|---|---|
| $P_{obs}$ | −0.0048 +/− 0.0028 | – | – |
| $P_{mod}$ | −0.0072 +/− 0.0007 | −0.0201 +/− 0.0019 | −0.0191 +/− 0.007 |
| P-$E_{mod}$ (land) | −0.0026 +/− 0.0004 | −0.0103 +/− 0.0012 | −0.0101 +/− 0.0004 |
| P-$E_{mod}$ (sea) | −0.0026 +/− 0.0009 | −0.0389 +/− 0.0024 | −0.0542 +/− 0.0010 |

These are based on GHCN precipitation ($P_{obs}$), an average of CMIP3 model-runs for land-precipitation ($P_{mod}$) and P-E (P-$E_{mod}$) averaged separately over land and sea. 95% confidence intervals are shown (From Mariotti et al. (2008))

### 8.1.3 *Observed Twentieth Century Changes*

CMIP3 simulations for the twentieth century suggest that the impact of greenhouse gases (GHG) increase (IPCC 2007a) may have already been manifesting itself in the Mediterranean region as a tendency toward drier and warmer conditions (Fig. 8.1). In this and following sections, diverse observational water cycle data is analyzed to compare CMIP3-simulated twentieth century GHG forced changes with observations, keeping in mind that natural (or internal) variability together with GHG increase may have contributed to observed variations.

Considering linear trends over the course of the twentieth century, a weak albeit significant long-term negative precipitation trend is found in both GHCN and DAI land data over the Mediterranean region (for GHCN this is −0.005 +/− 0.003 mm/d per decade; see Table 8.2 and Fig. 8.3); instead, CRU/PRECL data shows no trend, likely an artifact from combining two datasets. CMIP3 simulated precipitation trend is somewhat higher than that from GHCN or DAI data, possibly suggesting a tendency for the models to exaggerate future precipitation decrease. In all datasets, winter season precipitation shows a major downward deviation over the period 1960–2004 (−0.09 +/− 0.02 mm/d per decade), with interdecadal variations (a decrease during the period mid-1960s to early-1990s and an increase after that) largely related to the behavior of the North Atlantic Oscillation (Hurrell 1995). Dry season negative trends over the period 1950–2000 have also been observed in relation to a blocking-like pattern deflecting storms away from much of western and southern Europe (Pal et al. 2004).

The combination of the evaporation and precipitation changes described in previous sections resulted in significant long-term changes in Mediterranean Sea surface fresh water fluxes during the period 1958–2006 (Fig. 8.4).

Estimates based on OAFlux/REOFS suggest a substantial increase in E–P over this period (~0.5 mm/d in total). Considering the 1979–2006 sub-period, E–P rate of increase is estimated 0.1–0.3 mm/d per decade (see Table 8.3; estimates are mostly statistically consistent).

The E–P increase during the 1980s is primarily driven by the decrease in precipitation during this period. Similarly, the "dip" in E–P during the mid-1990s is also precipitation-driven, and is depicted quite consistently across data sources. In contrast, the most recent E–P increase is dominated by evaporation increase. The observational

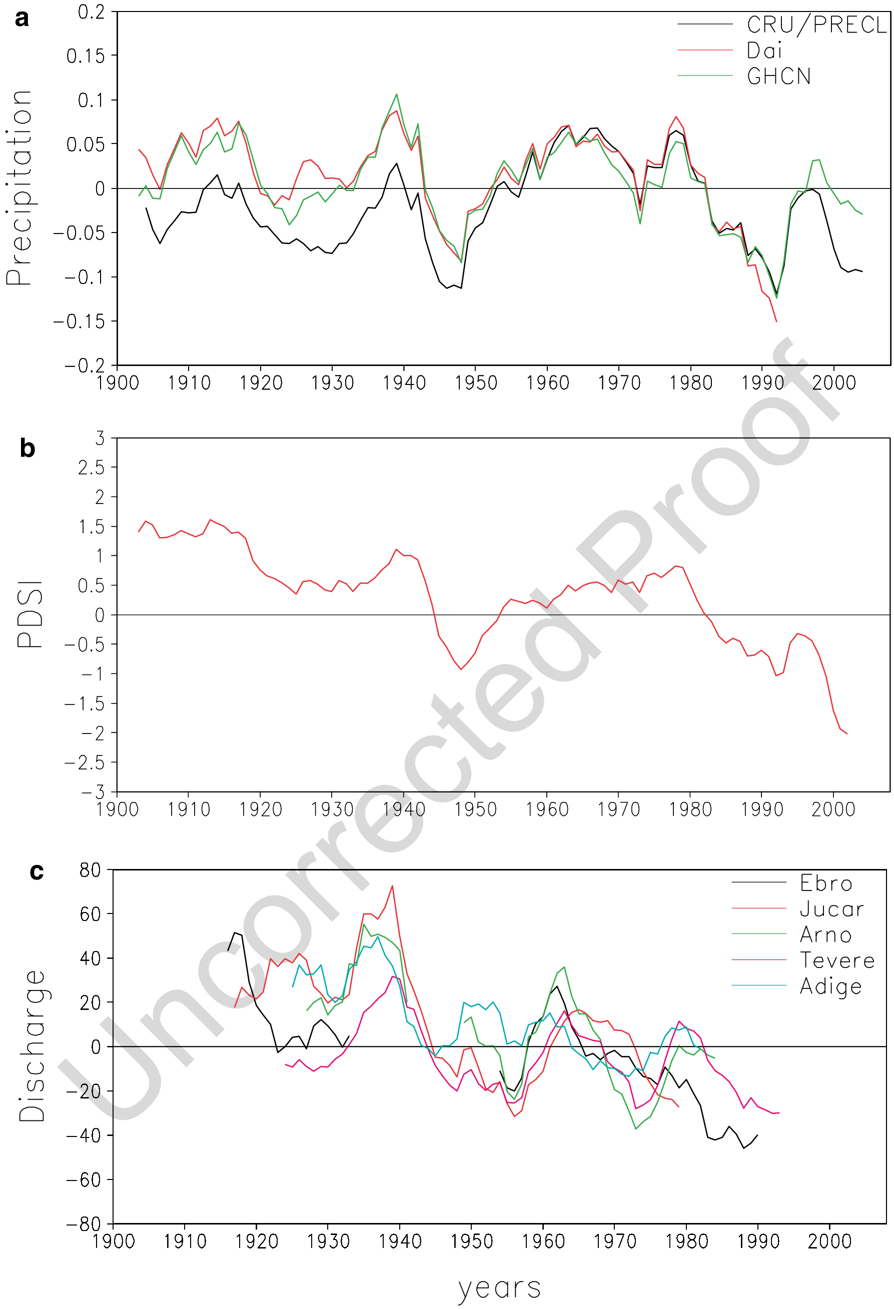




**Fig. 8.3** Mediterranean water cycle changes observed during the twentieth century relative to the period 1950–2000. Area-averaged annual mean precipitation anomalies (6-years running means) from various datasets (*panel a*; mm/d) and PDSI (*panel b*; a.u.); discharge anomalies (units are % of climatology) for various Mediterranean rivers (*panel c*). Due to data availability, discharge anomalies are relative to the 1960–1980 period (From Mariotti et al. (2008))

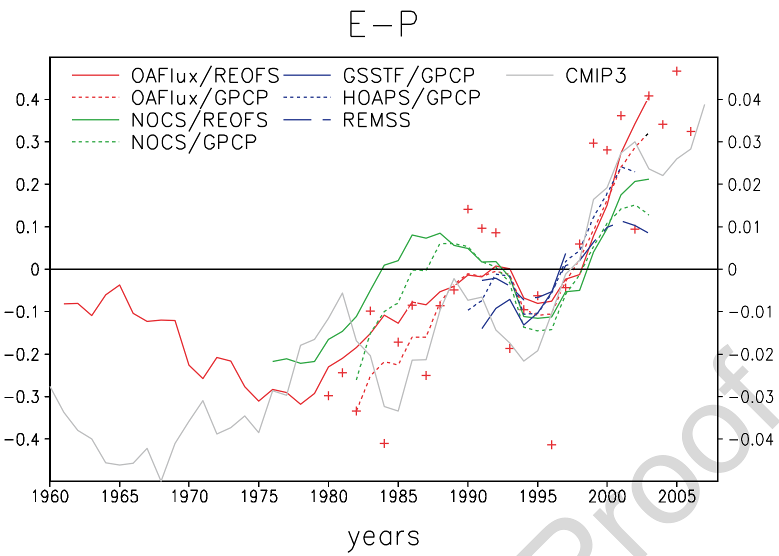


**Fig. 8.4** Observed decadal variations in Mediterranean Sea air-sea fresh water fluxes over the period 1958–2007. Shown are 6-year running means of area-averaged evaporation minus precipitation (E–P) anomalies relative to the period 1988–2000 (*lines*). Various observational sources are used (see legends; *left* hand scale). E–P estimates are derived combining precipitation estimates (PRECL, CRU and GHCN are land-only averages for the region surrounding the Mediterranean Sea; REOFS, GPCP and REMSS are Mediterranean Sea-only averages) with evaporation estimates (OAFlux, NOCS, HOAPS, REMSS, GSSTF). Annual mean values are also displayed (*symbols*) based on GPCP precipitation and OAFlux evaporation.CMIP3 models' ensemble running mean averages are also displayed (*grey line*; note different scale at *right*). Units are mm/d (Adapted from Mariotti (2010))

E–P results discussed here are broadly consistent with those from the CMIP3 simulations, with an overall tendency for Mediterranean E–P to increase during 1958–2006. However, CMIP3 E–P anomalies are about one order of magnitude smaller than observed.

During 1979–2006, annual mean E–P increased everywhere in the Mediterranean Sea and most substantially in the Ligurian Sea, Adriatic Sea and parts of Southeastern Mediterranean (up to 0.4–0.5 mm/d per decade based on OAFlux and GCPC estimates; not shown). Increases of 0.2–0.3 mm/d per decade were widespread. October to March means shows a similar pattern of increase but rates of increase are much higher (over 0.5 mm/d per decade) in vast parts of the Mediterranean. A similar analysis based on NOCS/GPCP, gives E–P trend patterns that are consistent with those described above except rates of change are generally more modest (maximum annual rates are 0.3–0.4 mm/d per decade).

In addition to the increase in sea-surface fresh water deficit described above, there is also evidence of a decrease in runoff into the Mediterranean Sea. The Palmer Drought Severity Index (PDSI), which reflects the combined effects of precipitation and surface temperature changes, shows a progressive and substantial drying of

**Table 8.3** Linear trends of annual mean evaporation (*E*), precipitation (*P*) and *E–P* (Parts **a**–**c**, respectively) for the periods 1958–2006 and 1979–2006 (mm/d per decade) using various data sources. Statistically significant results are in italic bold (From Mariotti (2010))

| | | 1958–2006 | 1979–2006 |
|---|---|---|---|
| **a** | **E** | | |
| | **OAF lux** | ***0.063 ± 0.039*** | ***0.235 ± 0.073*** |
| | **NOCS** | – | ***0.107 ± 0.058*** |
| | **CMIP3** | 0.003 ± 0.004 | ***0.011 ± 0.007*** |
| **b** | **P** | | |
| | **GPCP** | – | −0.046 ± 0.084 |
| | **REOFS** | ***−0.041 ± 0.032*** | 0.007 ± 0.078 |
| | **CRU** | ***−0.031 ± 0.023*** | −0.021 ± 0.071 |
| | **PRECL** | ***−0.036 ± 0.018*** | −0.033 ± 0.044 |
| | **GHCN** | −0.018 ± 0.025 | 0.006 ± 0.052 |
| | **CMIP3** | ***−0.011 ± 0.006*** | −0.009 ± 0.016 |
| **c** | **E–P** | | |
| | **OAFlux/GPCP** | **–** | ***0.276 ± 0.077*** |
| | **OAFlux/REOFS** | ***0.104 ± 0.046*** | ***0.228 ± 0.097*** |
| | **NOCS/GPCP** | **–** | ***0.148 ± 0.090*** |
| | **NOCS/REOFS** | **–** | ***0.100 ± 0.095*** |
| | **CMIP3** | ***0.014 ± 0.006*** | ***0.019 ± 0.014*** |



Mediterranean land surface over this region since 1900 (−0.2 PDSI units/decade) consistent with a decrease in precipitation and an increase in Ts (not shown). The interdecadal fluctuations are similar to those of precipitation, with wetter 1960s compared to the drier 1940s. Consistently, a number of Mediterranean rivers for which long-time series are available also show long-term decreases in discharge during the twentieth century. While such decrease could be in part due to intensified water use (time-series were not naturalized), we suspect an important contribution from the general drying trend suggested by the PDSI.

## 8.2 Evaluation of Atmospheric Moisture Budget for the Recent Climate Based on Super High-Resolution JMA Model

### *8.2.1 Introduction*

The Mediterranean Sea is a marginal and semi-enclosed sea. It is located in a transitional zone, where both mid-latitude and tropical dynamics play an important role (Alpert et al. 1990). The complex topography over the Mediterranean region yields a unique climate within this small area with steep gradients. Lack of water is a specific feature over this densely populated region, particularly over the Middle

East region. The trend of global warming makes the topic of water resources particularly sensitive over the Mediterranean (Ziv et al. 2005), as also reported by the Intergovernmental Panel on Climate Change (IPCC) Fourth Assessment Report (AR4) (IPCC 2007a). Therefore, a better understanding of the distribution of the atmospheric moisture budget components over this region is of great significance.

The dynamic factors which influence the moisture fields over the Mediterranean region are complicated. Except the regional small synoptic scale factors, earlier studies have shown that the climate of the Mediterranean region has significant teleconnections, such as the El Niño Southern Oscillation (ENSO) (Fraedrich 1994; Price et al. 1998; Diaz et al. 2001); variabilities of South Asian Monsoon and Africa Monsoon (Reddaway and Bigg 1996; Rodwell and Hoskins 1996; Chou and Neelin 2003; Ziv et al. 2004), as well as the large increase in Red-Sea trough frequencies (Alpert et al. 2004) and also Tropical Cyclones (Krichak et al. 2004). To better encompass all the factors into consideration, the climate model is an essential tool to study the future moisture budget and the water cycle changes over this area. Several studies concerning the climate change over the Mediterranean region based on several climate models have been carried out recently (Gibelin and Deque 2003; Alpert et al. 2008; Giorgi and Lionello 2008; Mariotti et al. 2008). Mariotti et al. (2008) (here after, MARIO) studied the water cycle changes over the Mediterranean region, by using data from the multi-model projections of the World Climate Research Program/Coupled Model Intercomparison Project Phase 3 (WCRP/CMIP3). They concluded that a transition to a drier twenty-first century is expected over the Mediterranean region, the result is also consistent with Seager et al. (2007) employing ensemble climate models. However, nearly all of the model data employed for the future climate studies are coarse resolution, with a typical horizontal spatial resolution greater than 100–200 km. Therefore, it is quite interesting to compare these results with a super-high resolution global grid climate model.

This study aims to perform a comparison study of the changes in the future moisture budget components over the Mediterranean region between MARIO results and those from a super-high resolution global climate model. Also, a brief study of predicted changes of Mediterranean Sea water discharge by using a river model is described.



## *8.2.2 Data and Methodology*

### 8.2.2.1 The Super-High Resolution Global Climate Model (GCM)

To study the climate changes over the Mediterranean region, a super-high resolution 20 km grid GCM developed at the Meteorological Research Institute (MRI) of the Japan Meteorological Agency (JMA), was employed. It is a climate-model version of the operational numerical weather prediction model used in the JMA. A detailed description of the model is given in Mizuta et al. (2006). The two runs of the 20 km

GCM cover the time periods 1979–2007 for current/control and 2075–2099 for the future. The control run used the observed monthly sea surface temperatures (SST) and sea-ice distribution, while the future run used the SST and sea-ice concentration anomalies of the multi-model ensemble projected by CMIP3 under the Special Report on Emission Scenario (SRES) A1B emission scenario. Details of the method are found in Mizuta et al. (2008). The JMA 20 km GCM data have been validated against past climate over the Middle East as well as over the Mediterranean region, details can be found in Kitoh et al. (2008a).

#### 8.2.2.2 The River Model

The river flow model in this study is the Global River flow model using the Total Runoff Integrating Pathways (TRIP) (GRiveT) developed at the MRI. TRIP is a global river channel network in a 0.5° by 0.5° grid originally designed by Oki and Sud (1998). The effective flow velocity is set at 0.40 m/s for all rivers following studies that use flow velocities ranging from 0.3 to 0.5 m/s (Oki et al. 1999). It should be noted here that flow velocities are not constant and can vary widely from 0.15 to 2.1 m/s (Arora and Boer 1999). In the process of simulation, GRiveT distributes the runoff water on the model grids into TRIP grids with a weight that is estimated by the ratio of the overlaid area on both grids. GRiveT then transports the runoff water to the river outlet along the river channel through TRIP. It should be emphasized that GRiveT does not account for any human consumption, i.e. irrigation, dam or natural losses, i.e. infiltration, of the river water, which might cause some differences between the model and the observed river flow, as noted, for instance, with the Nile river flow in Egypt as analyzed later.

Two time periods monthly mean of the climatological river model data were investigated in this study: the control/current run (1979–2003) and the future projection (2075–2099).

#### 8.2.2.3 Study Area and Season

Following MARIO, a domain that covers the Mediterranean, Middle East, Europe and North Africa, was selected to investigate the large scale moisture budget components changes. It was defined by the latitude 20°–60°N and longitude 20°W–70°E with a total area approximately $3.1 \times 10^7$ km$^2$. The Mediterranean Sea covers the domain 10°W–40°E and 28°N–47°N with the total area of water body of about $2.5 \times 10^6$ km$^2$. In addition, the Mediterranean Sea was sub-divided into the west and east of Mediterranean Sea region at the 15°E longitudinal line in order to study moisture budget for the two sub-basins separately. The wet season was defined as from October to March, and the rest of the year (April to September) as the dry season.

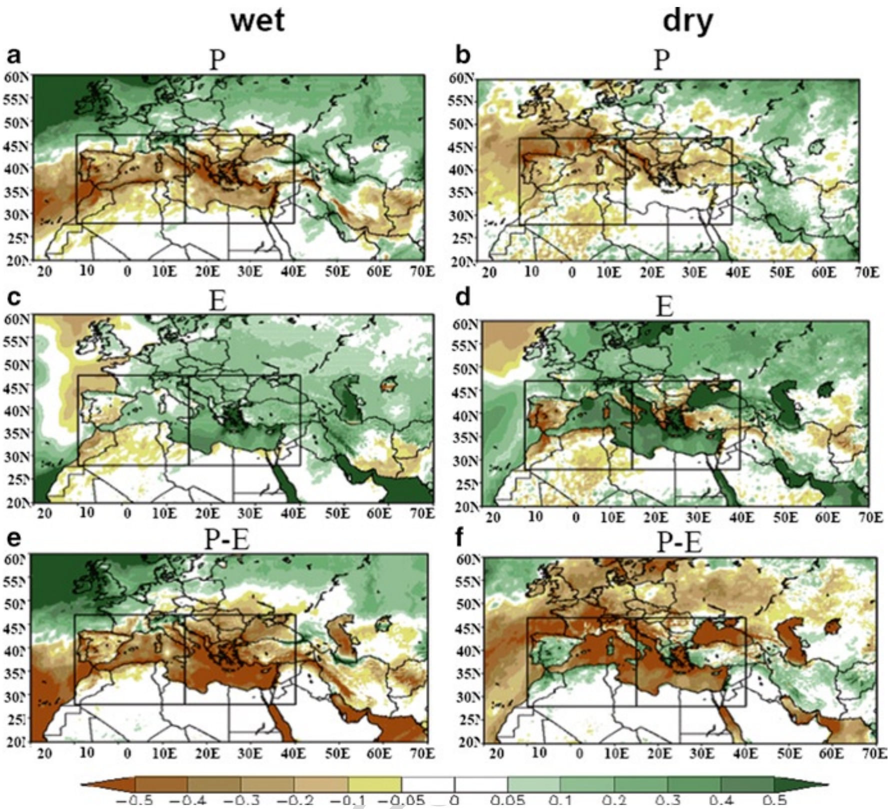


**Fig. 8.5** Mediterranean water cycle changes by 2075–2099 compared to 1979–2007 for the ‘wet’ and ‘dry’ seasons based on MRI 20 km GCM. Precipitation (**a**) and (**b**), evaporation (**c**) and (**d**), and precipitation minus evaporation (**e**) and (**f**). Unit: mm/day. The box broadly depicts the western and eastern Mediterranean region



### *8.2.3 Results and Discussions*

#### 8.2.3.1 Seasonal Moisture Fields Changes over the Large Domain

The seasonal change of the area mean evaporation (E), Precipitation (P) and P-E between the future and control runs (future minus control) over the large domain results based on the 20 km GCM are shown in Fig. 8.5.

In general, our results are very close to those of MARIO. During the wet season (left panels), three belts of changing precipitation can be identified clearly from south to north (Fig. 8.5a), which are with no significant change, decrease and increase of precipitation. These three belts are located below 30°N, 30°–42°N and above 42°N, respectively. The peak of precipitation decrease is located at the northern boundary of eastern Mediterranean Sea with a magnitude of over 0.5 mm/day (about 100 mm/ season). Jin et al. (2009) investigated the moisture budget over the Middle East by

**Table 8.4** Mediterranean mean evaporation (*E*), precipitation (*P*) and precipitation minus evaporation (*P*–*E*) anomalies in future (2075–2099) relative to current (1979–2007) separated by the sea and land areas

| Area | Parameters | Annual | Wet season | Dry season |
|---|---|---|---|---|
| Sea | E | 9.3%/0.35 | 5.7%/0.24 | 13.6%/0.45 |
| | P | −11%/−0.19 | −10%/−0.24 | −11.4%/−0.12 |
| | P–E | −26.2%/−0.54 | −25.4%/−0.48 | −25.4%/−0.57 |
| Land | E | −3.6%/−0.04 | 1.4%/0.01 | −5.8%/−0.09 |
| | P | −10%/−0.14 | −10%/−0.14 | −9.2%/−0.12 |
| | P–E | −43.5%/−0.10 | −21.7%/−0.15 | −13%/−0.03 |

In each column, relative (%, left) and absolute (mm/day, right) values are reported based on a 20 km global climate model

using 20 km GCM data, and demonstrated that the 20 km GCM credibly simulates the current precipitation regime over the eastern Mediterranean region.

Comparing the present and future simulations, during the dry season, as compared with the wet season, the belt of precipitation decreases moves a bit to the north (Fig. 8.5b), probably due to the northward shift of Hadley Cell. Detailed discussion of poleward widening of the Hadley Cell based on the different datasets can be found in Held and Soden (2006), Lu et al. (2007) and Johanson and Fu (2009). They also discussed some differences in the Hadley Cell expansion as seen in the observations and reanalysis data. This causes most of the southern and central European countries, which are adjacent to the Mediterranean Sea, to become drier in summer season in the future. For the change of the evaporation, E, both wet and dry seasons show a similar pattern (Fig. 8.5c, d). However, a significant difference can be found over the north Mediterranean coast, i.e. an increasing E during the wet season (Fig. 8.5c) but decreasing E during the dry season (Fig. 8.5d). As expected, all the water bodies show evaporation increases consistent with the sea surface temperature and air temperature increases, based on A1B emission scenario. The change of the net moisture budget, i.e. P-E, for both wet and dry seasons, shows that the Mediterranean Sea becomes drier (Fig. 8.5e, f). A major difference is that, the P-E is projected to decrease during the wet season, but increase during the dry season over the north Mediterranean coast. This could be the consequence of changes in E over the same area as discussed above. This finding cannot be identified in MARIO. In addition, limited by the spatial resolution, the change of P, E and P-E for the famous "fertile crescent" which is located at the Middle East, can be easily identified in the 20 km GCM, but is not clear in MARIO, as earlier suggested by Kitoh et al. (2008a).

Table 8.4 shows the projected future changes of the mean P, E and P-E, separated for annual, wet and dry seasons, and also for the land and sea bodies over the Mediterranean region. When compared with MARIO (MARIO results are in parentheses), the annual changes of P for sea and land from 20 km GCM are −11% (−15%) and −10% (−15.5%) respectively. The smaller decreases in P in this study are perhaps due to the different time periods for the control run used between these two studies, which are 1979–2007 and 1950–2000, respectively. Indeed the climatic period of 1950–1979 was somewhat different than the more recent decades due to inter-decadal variations.

The annual changes of E for sea and land areas are 9.3% (7.2%) and −3.6% (−8.1%). The reason for the big difference in E–changes over land between these two studies might be the different features of models used in each study. However, the annual projected changes of P-E for the sea body is quite close, i.e., −26% (−24%). For the wet season, the projected changes of P, E and P-E in these two studies agree quite well, both qualitatively and quantitatively, except for the change of E over the land area. For the dry season, in contrast, there are distinct differences in the projected changes of E and P. These differences also result in the annual differences between these two studies as discussed above. Another factor contributing to the differences between the two studies comes certainly from the very different spatial resolutions of the models. However, it is hard to figure out explicitly which factor is the key one in determining these differences.

#### 8.2.3.2 Changes of Monthly Running Means of E, P and P-E Over the Mediterranean

Figure 8.6 shows the seasonal cycle (3 months running mean) of E, P and P-E for the sea and land areas separately. Again, the results generally fit MARIOs, especially for the sea area (Fig. 8.6a). However, there are some interesting differences. For instance, the simulated summer P over the land area from the 20 km model is larger than that of MARIO, by a factor of about two (Fig. 8.6b). The same analysis by using the climate research unit (CRU) data, which are derived from the observations, exhibits a similar pattern to MARIO, but somewhat over estimated the precipitation for the winter season (Fig. 8.6b). It seems that the 20 km run overestimates the summer P of land area. A plausible explanation is that, the total land area over our research is relatively small, and the topographically forced precipitation has a significant influence over the complex water-land region, particularly in the summer as the local forcing plays an important role in precipitation genesis. On the other hand, no significant difference of land precipitation in the winter was found between these two studies, probably due to the fact that winter precipitation is mostly influenced by the synoptic systems. Jin et al. (2009) showed that, compare to CRU, the 20 km GCM has a better performance in capturing the land area precipitation. Hence, the coarse resolution models seem to be unable to capture the detailed precipitation information over such a small land area, i.e. only several grid points data can be obtained from the coarse data. The P-E curves suggest that both the land and the sea area of Mediterranean region will become more arid in the future, and the sea area will be experience even greater decreases in precipitation than the land area.

#### 8.2.3.3 Comparing West and East Mediterranean

The quite different geographical positions of the western (WMS) and the eastern Mediterranean Seas (EMS), which neighbor the huge moist Atlantic Ocean on the west and the arid Middle East on the east respectively, make it interesting to compare the moisture budgets in both.

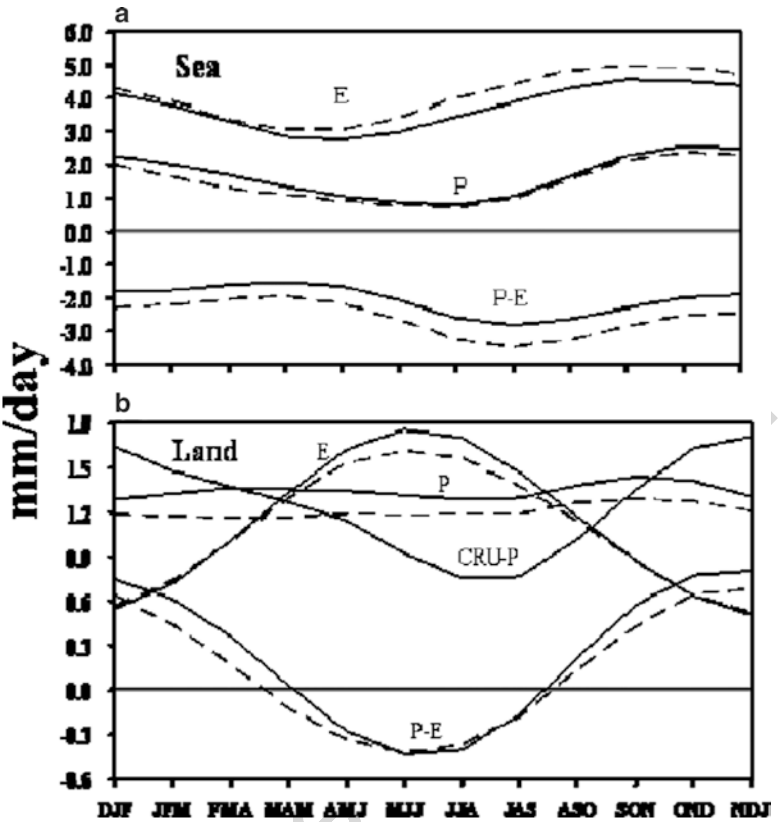


**Fig. 8.6** Mediterranean water cycle in 1979–2007(*solid*) compared to 2075–2099 (*dashed*) based on the MRI 20 km GCM. The seasonal cycles (3 months running mean) of precipitation (*P*), evaporation (*E*) and precipitation minus evaporation (*P-E*) are shown (mm/day). The same CRU precipitation for 1979–2002 is added for comparison. (**a**) Sea-only (**b**) Land-only



Figure 8.7a shows not surprisingly, that the current (present climate) evaporation of the EMS is higher than that of WMS, with annual average values of 3.9 and 3.5 mm/day, respectively. This is probably due to the EMS being closer to the hot climate of the arid Middle East as well as the Indian monsoon, leading to significant subsidence over the EMS in summer as reported by Rodwell and Hoskins (1996) and further discussed by Ziv et al. (2004). It should be also noticed that the maximum evaporation for the EMS and WMS appears during the winter and autumn seasons. This result is consistent with Jin and Zangvil (2009), who employed NASA reanalysis data. For the current precipitation, except for the central winter season (Dec-Jan), the average EMS precipitation is lower than the WMS (Fig. 8.7a), with the mean annual value of 1.5 and 1.8 mm/day, respectively. This result is probably related to the WMS receiving more moisture from the Atlantic Ocean than the EMS area. Another reason is that the northern part of the WMS is further north and therefore closer to the baroclinic zone. The P-E of the current day run for the EMS and WMS again indicates that the EMS is significantly drier than the WMS, especially during the summer and the autumn seasons (Fig. 8.7a).

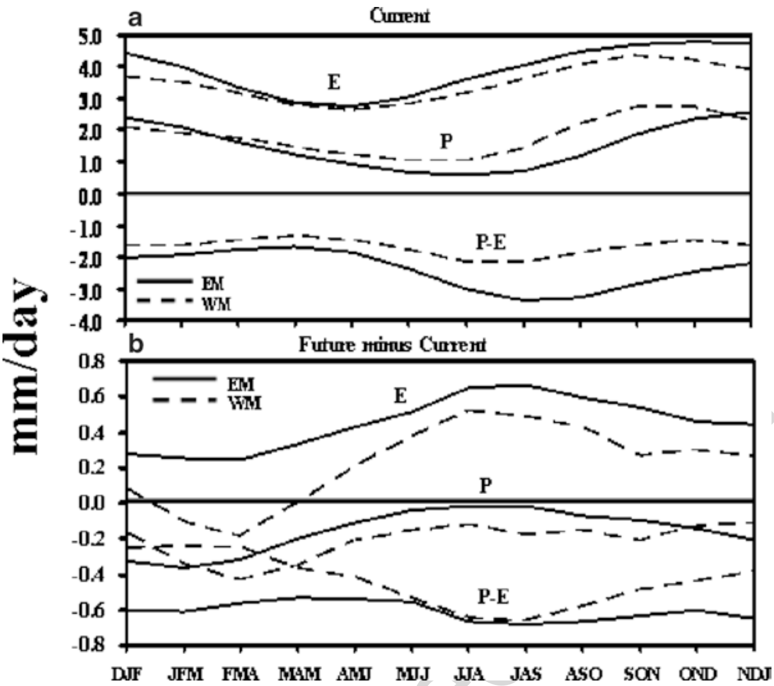


**Fig. 8.7** Sea area water cycles for western Mediterranean (*dashed*) and eastern Mediterranean (*solid*) based on MRI 20 km GCM. The seasonal cycle (3 months running mean) of precipitation (*P*), evaporation (*E*) and precipitation minus evaporation (*P-E*), is shown (mm/day). (**a**) Current (1979–2007) (**b**) Future (2075–2099) minus current

Figure 8.7b shows the model projected changes of P, E and P-E over the water body of the EMS and the WMS between 1979–2007 and 2075–2099. The E changes show a dominant increasing E trend for both regions, except for some decrease of E for the WMS in the spring (March). The magnitude of E increase in the EMS is higher than that of the WMS, with the average values of +0.45 and +0.22 mm/day, respectively. It is not clear why an E decrease is projected in the spring season for the WMS in the future. Another finding is that in spite of projected P-decrease in both the EMS and the WMS, the magnitudes in the WMS are higher than that of EMS with the mean value of −0.21 and −0.16 mm/day, respectively, except for the winter season (Fig. 8.7b). However, P-E still shows that the EMS becomes drier than the WMS in the future, with mean values of P-E changes, −0.61 and −0.43 mm/day, respectively. That means, that the already drier EMS is projected to become even drier compared to the WMS.

#### 8.2.3.4 Change of River Discharge over Mediterranean Region

In order to obtain a more complete picture of the water cycle budget for the Mediterranean region, it is interesting to examine the projected changes of river discharges, although it has a close relation with the precipitation regime, especially for those main rivers flowing into the Mediterranean Sea.

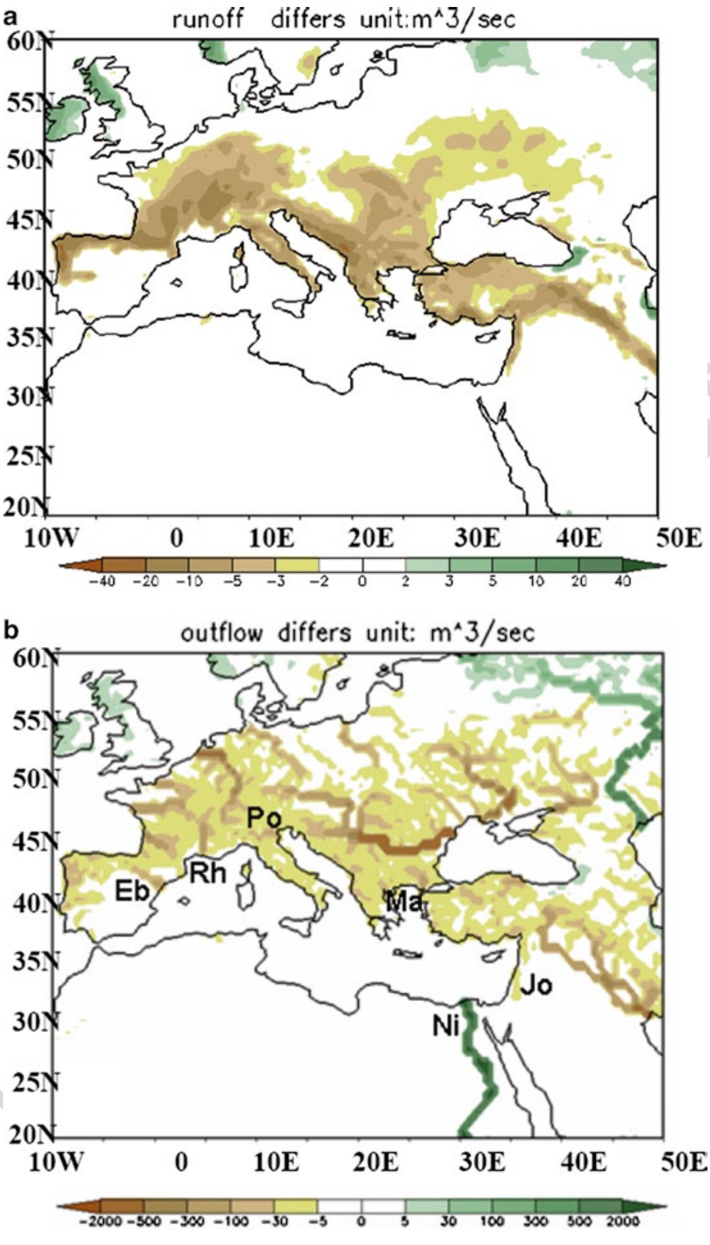


**Fig. 8.8** Changes of runoff and river discharge by 1979–2003 compared to (2075–2099). (**a**) runoff (**b**) river discharge. Six rivers are marked as Ebro (Eb), Rhone (Rh), Po (Po), Maritsa (Ma), Jordan (Jo) and Nile (Ni). Unit: ($m^3$/s)

Figure 8.8 shows the changes in the runoff over land and the changes in the river flow rates between future (2075–2099) and current (1979–2003) periods based on the MRI river model. Figure 8.8a shows a clear decrease of the runoff over the continent of the north Mediterranean region with a mean value of approximately −10 $m^3$/s, primarily as a result of the decreasing precipitation in the region. As a consequence, the flow rate of most of the rivers over this area is decreasing (Fig. 8.8b). It is interesting to note that the river model also shows that the Nile River is projected to have an increased flow rate in the future. This is due to the projected increase in rainfall in the tropics discussed in detail by Kitoh et al. 2008a.

To further investigate the change of river discharge, several large rivers flowing into the Mediterranean Sea, were selected in a similar manner to MARIO. The rivers' names and the countries where the estuaries are located are as follows: Ebro in Spain; Rhone in France; Po in Italy; Maritsa in Turkey; and the Nile River in Egypt. In addition, the Jordan River, as the only river which does not flow into the Mediterranean was selected in order to examine its change of flow rate at the estuary of the Dead Sea. The reason for doing this is that the Jordan River is not only the main water resource for the bordering countries in the East Mediterranean, but also a significant influence on the water balance of Dead Sea, and hence on life in this sensitive region.

Instead of calculating the mean flow rate of the rivers, only the flow rates at the estuaries for each river was examined because of our great concern for the potential variations in the river discharges into the Mediterranean Sea.

Figure 8.9 shows that except for the Nile River, a decreasing trend of monthly mean river discharges is projected for the future. The most dramatic decrease of river discharge is found for the rivers Ebro, Maritsa and the Jordan River. The decreasing magnitude of the annual average discharge for the rivers Ebro, Rhone, Po, Maritsa and the Jordan River are 108, 307, 146, 184 and 19 $m^3$/s, corresponding to percentages of 46, 26, 18, 54 and 85% respectively. The decrease of discharge for the EM rivers Maritsa and the Jordan River is particularly large, i.e., even more than a half compared to the current rate. It should be mentioned here that, compared to the observed data, the current simulation of river discharge by the river model shows similar seasonal course from month to month. For instance, the Ebro River peaks in Mar/Apr and gets its minimum in Jul/Aug. However, the results from the river model underestimate the flow rate by a factor of two compared with the observed data except for the Nile River, where the deviation is much larger. Possible explanations for the error might be the simplified river model, which relies on the model estimation of the runoff, and the still relatively coarse spatial resolution of the river model. This error can be reduced to some degree when we focus on the difference of the river discharge between the future and the current. For further discussion on the Nile results see Kitoh et al. (2008b).

An increasing trend of discharge with the value of about 2,090 $m^3$/s was calculated only for the Nile. It should be also noticed here that the river model does not take into account any anthropogenic influences into the model consideration. Therefore, there are additional discrepancies for the river discharge between the model and observed data. For example, the river discharge for the river Nile from

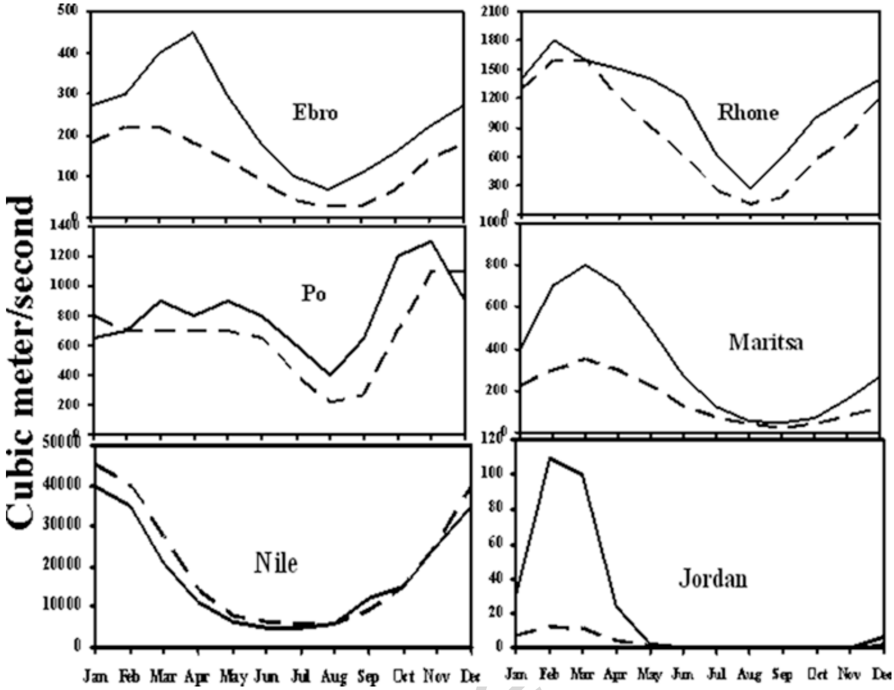


**Fig. 8.9** Changes of monthly mean river discharge of six rivers by (1979–2003) compared to (2075–2099). Except to the Jordan River, all rivers flow into the Mediterranean ($m^3/s$). *Bold lines* (▬▬▬▬) are for current climate, while *dashed* (▬ ▬ ▬) for the future



the model is higher than the observed data due to the huge Aswan dam constructed across the river in Egypt (Kitoh et al. 2008b). In addition, the Nile is the largest river that flows into the Mediterranean, and it has a crucial role in the balance of the river discharges in the Mediterranean. However, as the model showed, the absolute value of increasing discharge from the Nile River only, is larger than the sum of all decreasing discharges from the other four rivers. Hence, it may seem that an overall surplus of river discharge was projected by this analysis. But, we should keep in mind, except the model errors mentioned above that there are numerous other small rivers over the European continent and isolated islands that flow into the Mediterranean, and all of those rivers are projected to experience a decrease in their discharge (Fig. 8.8b).

In agreement with this study, the MARIO study showed the decrease in river discharges for some rivers based on the observed data. Therefore, a future water deficit is projected over the Mediterranean. Moreover, research has shown that the salinity of the Mediterranean is increasing steadily from the observed data even in the recent decades (Millot et al. 2006). These results might caused by the combined effect of decreasing P, increasing E and the deficit water discharge in the Mediterranean region.

### 8.2.4 Summary

The JMA 20 km grid global climate model data were introduced to make a comparison study with Mariotti et al. (2008) of the water cycle components over the Mediterranean region. On a large spatial scale, results from these two studies are similar to each other, but there are some important differences. Precipitation future decreases are projected by both studies, but the drop of precipitation both for land and sea from the 20 km resolution model is not as high (4% lower) compared to MARIO's for the annual time scale. The seasonal cycle of precipitation, evaporation and precipitation minus evaporation over the land and sea area of the Mediterranean region from these two studies are similar. On the other hand, there are some significant differences between these two studies. For example, the water cycle change over the famous "fertile crescent" that is simulated quite well by the 20 km run compared to the coarser MARIO model; and the summer seasonal cycle of precipitation from the 20 km run, which is larger than in MARIO, by a factor of about two. The comparison of the water cycle over the water bodies of the western and the eastern Mediterranean show that for the current climate, the evaporation of the eastern Mediterranean is higher than that of the western Mediterranean with an average value of 0.4 mm/day, with the opposite true for precipitation, i.e. less than in the WMS with an average value of 0.32 mm/day. For the future, the evaporation increases over the eastern Mediterranean are higher than for the western Mediterranean, with the average values of 0.45 and 0.22 mm/day respectively. The precipitation future decreases for the western Mediterranean are higher than that for the eastern Mediterranean, with the average values of −0.21 and −0.16 mm/day. The change in precipitation minus evaporation (P-E), shows that the eastern Mediterranean becomes even drier than the western Mediterranean.

Results from the river model indicate that most of the rivers over the north Mediterranean region decrease their flow rate in the future. Further study for some key rivers which flow into the Mediterranean Sea shows that, some rivers, such as the Ebro in Spain, and the Maritsa in Turkey, become much drier in the future. Notably, the discharge of the Jordan River to the Dead Sea decreases by a very high value of 85% projected by the model.

It can be concluded from these two studies that a drier climate transit might be inevitable over the Mediterranean by the end of twenty-first century. Hence, a water crisis may become a big challenge in the future for the study area.

## 8.3 Multi-model Changes in Evapotranspiration, Precipitation and Renewable Water Resources

### 8.3.1 Introduction

The increases in temperature that are projected to occur right across the Mediterranean region over the coming decades will impact upon all aspects of the region's hydrological cycle and hence upon the potential available water resources in this highly water-sensitive region. To make assessments of how the water resources around the Mediterranean basin may change in the future as a result of climate change, it is necessary to consider the inputs and outputs of the system and how they may interact to affect runoff.

The IPCC Fourth Assessment Report describes a high degree of consensus between the global climate model (GCM) projections of change over the Mediterranean (IPCC 2007a WG1 Chapters 10 and 11; IPCC 2007b WG2 Chapters 9 and 12), not only in temperature change, but in precipitation and other aspects of the hydrological cycle. Generally, the GCMs are indicating warmer and drier conditions to come as we move through the twenty-first century. However, uncertainty in the projections is acknowledged, particularly in the model representation of large-scale modes of variability that affect Mediterranean climate such as the North Atlantic Oscillation, and how these may change in the future.

Global models provide large-scale patterns of change over the region, but the current generation of GCMs cannot be expected to represent the fine detail required for impacts assessments. The Mediterranean is a geographically complex region in its distribution of land and sea, as well as topography. Regional or enhanced-resolution climate models provide an important means by which possible finer-scale changes can be assessed. The uncertainties in patterns, magnitude and timing of the large-scale changes simulated by the global models are transferred to the regional climate models (RCMs) through the boundary conditions. The RCMs then add a further layer of complexity in their finer-scale representation of the topography and coastline, and features of the weather and climate. Therefore, even in a region where there is general consensus between the global models, it is essential to consider a range of regional climate model projections of change. Of course, consensus does not in itself imply confidence, although for the Mediterranean region many of the features and changes in climate simulated by the GCMs are understood physically. To drive understanding both of how the regional climate may respond to increasing greenhouse gases in the atmosphere and how the models simulate the changes, it is advisable to look at a number of models if possible. Through the CIRCE project and associated activities, output from a number of high-resolution models has been made available for analysis.

This section reports on five climate model projections of changes in aspects of the hydrological cycle for the Mediterranean region. Three of these models have an interactive Mediterranean Sea, and two are versions of the Met Office Hadley Centre regional model with different land surface schemes (see below). The focus is upon changes in evapotranspiration, and how these changes could be important in controlling available renewable water resources (runoff). It will highlight areas of consensus between the models, and areas of disagreement.

### *8.3.2 Models and Methods*

The regional models used in this study are as follows: ENEA (Italian National Agency for New Technologies, Energy and Sustainable Economic Development), MPI-HH, (hereafter referred to as MPI; Max Planck Institute for Meteorology), and the HadRM3-MOSES1 and HadRM3-MOSES2 (Met Office Hadley Centre). In addition, the output from the Météo-France model was used, which is a global model with enhanced resolution over the Mediterranean region. The ENEA, MPI and Météo-France models are described in detail in Part1 of this Book. The HadRM3 models are not described there, and so a description follows here.

HadRM3 is the UK Met Office Hadley Centre's regional climate model. Nested within the HadCM3 global model, it was run over the Europe domain – including the Mediterranean – at a spatial resolution of approximately 25 km. Global model HadCM3 (Gordon et al. 2000) has an atmospheric resolution of 2.5° latitude × 3.75° longitude and 19 levels the in the vertical, while the ocean has 20 levels at 1.25° latitude × 1.25° longitude resolution. The versions of HadRM3 used in this study were based on the same global model as used to provide the driving boundary conditions, with consistent parameter settings. Simulations ran over the 1960–2050 CIRCE time frame under the SRES A1B emissions scenario. The two versions of HadRM3 differ in their land surface scheme, which was updated from MOSES1 (Met Office Surface Exchange Scheme version 1, Cox et al. 1999) to MOSES2 (version 2, [AU4] Essery et al. 2003). The original land surface scheme, MOSES1, represents each grid box as an area-average land surface type (calculated from observations) and associated physical exchanges and parameterizations are also calculated as area-weighted averages. In order to improve the variations in the land surface types, the Met Office developed a "tiled" surface scheme, MOSES2, which allows for sub-grid scale variations at the model surface. Each model grid box is composed of a varying mix of nine surface types (five vegetation and four non-vegetation). The transport of heat and water is then calculated explicitly for each surface type, and then averaged using blending height techniques to give grid box values. This constitutes an improved treatment of the surface exchanges.

For ease of comparison, the models were all placed on a regular latitude-longitude grid, which required regridding in most cases. Where regridding was necessary, the size of the gridboxes was kept close to the native resolution. The global Météo-France model had the coarsest resolution of the models under analysis here, at 0.5° latitude-longitude, and the other four models were regridded to a 0.25° latitude-longitude grid. The same domain was extracted for each model (10°W–41°E; 27°N–49°N) for further analysis. Some modification to the data would have taken place through the regridding process, but the focus of this analysis is primarily on broad patterns of change, which should not be affected.

The majority of the results presented here are based on analysis of differences between future decadal means up to 2050 relative to a 30-year baseline climatology (1961–1990). This allows the largest signal owing to climate change to be displayed, although it should be noted that the decadal means are more subject to the noise of interannual climate variability.

Due to some inconsistencies in the diagnostics available for each model, the evapotranspiration variable has been taken from the ENEA model, while from the other models, the latent heat flux, converted to a moisture flux (mm/day) using the latent heat of vaporization, was used as a proxy for evapotranspiration.

### *8.3.3 Spatial Changes in Precipitation and Evapotranspiration*

The maps in Figs. 8.10a, b show annual and seasonal 2041–2050 anomalies relative to the 1961–1990 baseline for precipitation and evapotranspiration, land areas only. On the broadest scale, they are consistent with the changes projected in the AR4 models, for a move towards reduced rainfall and evapotranspiration by the middle of the twenty-first century.

At the annual mean scale (Fig. 8.10a), the models show a fairly consistent picture of reductions in rainfall around the Mediterranean, particularly in the Iberian peninsula, North Africa of the western basin, parts of southern France, Italy, parts of Greece, western and southern Turkey, and coastal Middle East. There are also some regions of model disagreement in the sign of the change, including northern Turkey, the coastline from Croatia to Albania, and parts of southern France. But even where models agree in the sign of the change, there are variations in the magnitude. The two HadRM3 models and the MPI model project larger changes than the other two models. In general, anomalies in all aspects of the water cycle in the Météo-France model are smaller than the other models. This is likely to be related in part to the coarser resolution of this model, which does not produce the high rainfall associated with the complex orography that is better represented in the finer resolution models (Hemming et al. 2010). In addition, the temperature response to increased atmospheric greenhouse gases is not as large in the Météo-France model, and therefore the response by the hydrological cycle would likewise be expected to be lower magnitude. During the winter, there is a broad north-south split in the sign of the change, at least in the ENEA and the two HadRM3 models, with wetter conditions to the north and drier to the south. There is general consensus between the models that the greatest declines in rainfall around the Mediterranean are projected for the spring and summer seasons. Excluding the very dry desert areas, the largest percentage decreases are projected for southern Spain, Italy (excluding the Météo-France model, in which changes are relatively small and mixed in sign) and southern and western Turkey. These patterns of change are broadly consistent with those found in the high-resolution JMA model described in Sect. 8.1.2. Rainfall is projected to decline across large areas by over 20% in all of the models, although in the Météo-France model, the central part of the northern Mediterranean domain, such as over southern Italy and Greece, has areas of increase as well as decrease. In pockets of Turkey, the eastern Mediterranean, Italy and Spain, projections from the MPI, HadRM3-MOSES2, HadRM3-MOSES1 and ENEA models are for decreases in summer rainfall of 50% or more.

The pattern of change in annual mean evapotranspiration (Fig. 8.10b) by the 2040s relative to the baseline is similar to, but smaller in magnitude than, the precipitation changes. Where projections are for reductions in rainfall, evapotranspiration also declines. Winter anomalies are small while cooler temperatures keep evapotranspiration at low levels. But as temperatures build during spring and evapotranspiration increases, larger anomalies can develop. There is inter-model consistency in the pattern of anomalies across the domain with greater evapotranspiration

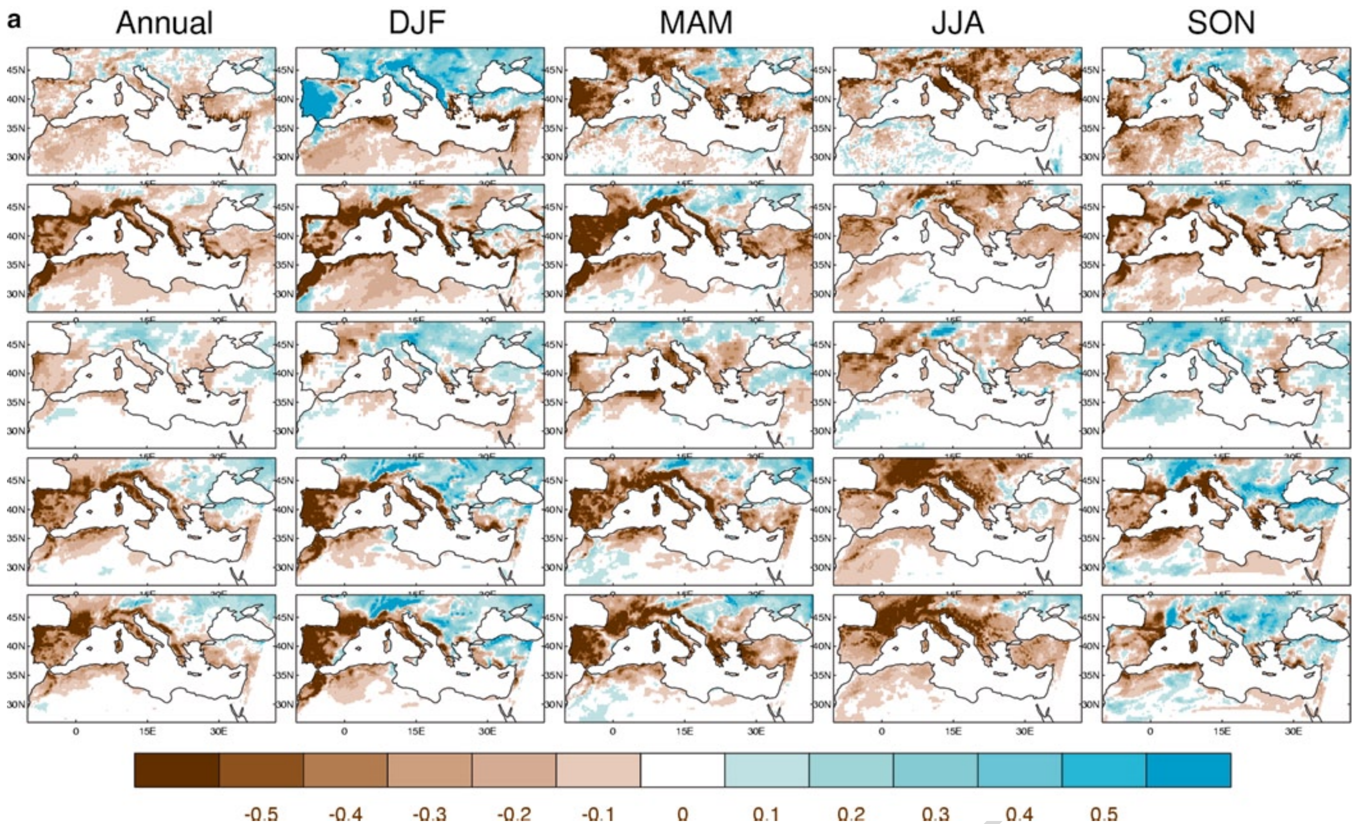


**Fig. 8.10** (**a**) ΔPrecipitation. Annual and seasonal 2041–2050 anomalies relative to the 1961–1990 *baseline* (mm/day). Row 1: ENEA; row 2: MPI; row 3: Météo-France; row 4: HadRM3-MOSES1; row 5: HadRM3-MOSES2. (**b**) ΔEvapotranspiration. Annual and seasonal 2041–2050 anomalies relative to the 1961–1990 *baseline* (mm/day). Row 1: ENEA; row 2: MPI; row 3: Météo-France; row 4: HadRM3-MOSES1; row 5: HadRM3-MOSES2. (**c**) ΔPrecipitation

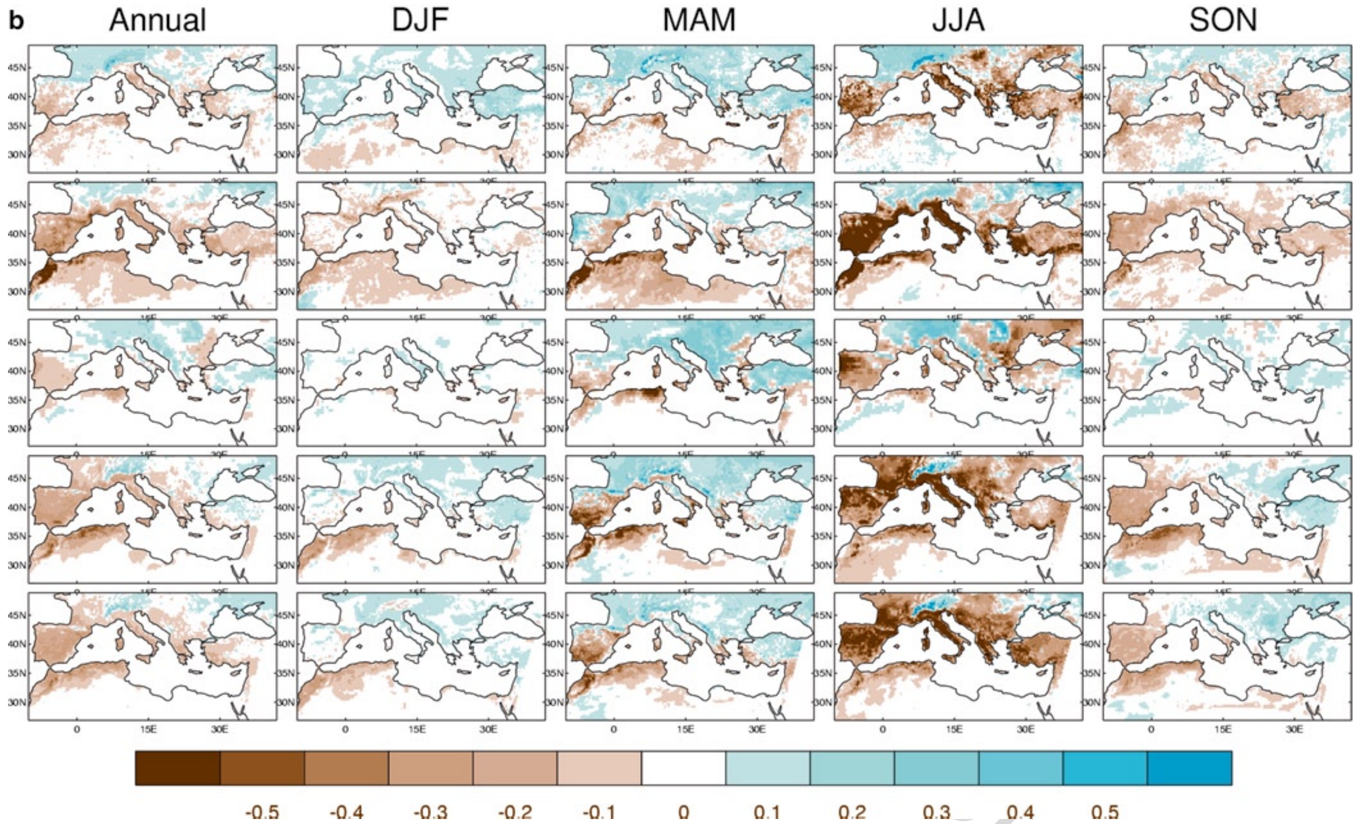


**Fig. 8.10** (contiuned) – ΔEvapotranspiration. Annual and seasonal 2041–2050 anomalies relative to the 1961–1990 *baseline* (mm/day). Row 1: ENEA; row 2: MPI; row 3: Météo-France; row 4: HadRM3-MOSES1; row 5: HadRM3-MOSES2. (**d**) ΔRunoff. Annual and seasonal 2041–2050 anomalies relative to the 1961–1990 *baseline* (mm/day). Row 1: ENEA; row 2: MPI; row 3: Météo-France; row 4: HadRM3-MOSES1; row 5: HadRM3-MOSES2

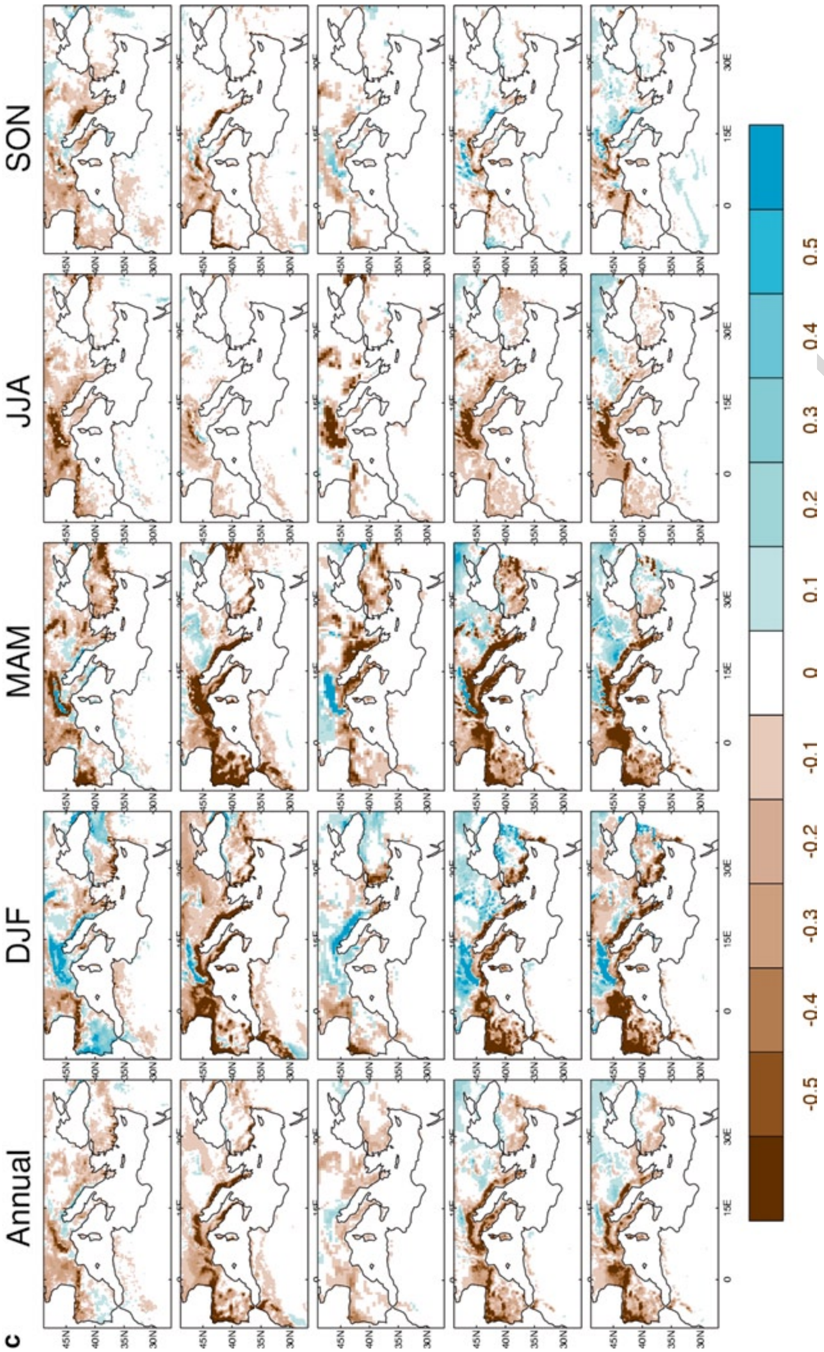


**Fig. 8.10** (contiuned)

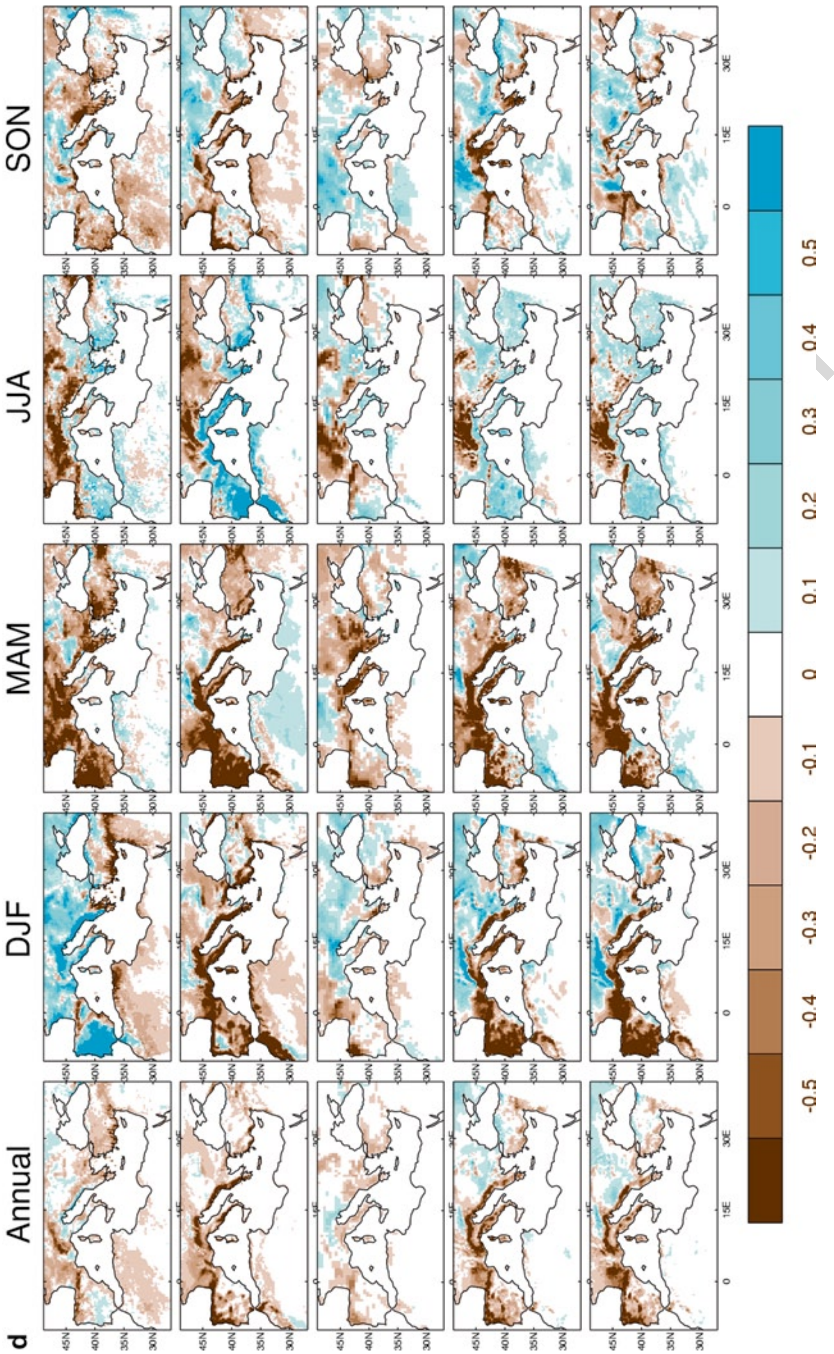
d
Annual
DJF
MAM
JJA
SON
-0.5
-0.4
-0.3
-0.2
-0.1
0
0.1
0.2
0.3
0.4
0.5

to the north, probably related to the increasing temperatures, and lower to the south. This pattern is replaced during summer with more widespread and much more intense reductions in evapotranspiration around the Mediterranean Sea, particularly on the northern side. Increases in evapotranspiration persist further north. These summer patterns of change are again similar to those simulated by the high-resolution JMA model (Sect. 8.1.2). The HadRM3 models display the most widespread and some of the higher magnitude reductions, but there are strong reductions in the MPI model as well, particularly in the Iberian Peninsula, the coast of southern France, Italy, western Turkey and Morocco. Again, there is a more mixed picture presented by the Météo-France model, with some parts of the region, such as the Croatia to Greece coastline, projecting increases in evapotranspiration. However, there are regions such as Italy, the Iberian Peninsula and parts of North Africa and Turkey that show consistent decreases across all models.

### *8.3.4 Hydrological Controls on Water Resource*

In such a water-sensitive region, understanding how water resources may change over the next decades is of critical importance. By examining runoff in the models, and the relationships between system inputs and outputs – precipitation and evapotranspiration – a number of objectives can be achieved. We can analyze how these quantities are projected to change and therefore gain understanding of what is controlling the changes in runoff. In addition we can compare the models, improving understanding of how the models are simulating the hydrological cycle and helping to identify areas where model development is required.

By considering the ratio between the evapotranspiration and precipitation (E/P ratio), we can assess which is the dominant control over runoff – the renewable supply of water – through the year, and how this may change in the future. There is strong inter-model agreement that during the majority of the year, precipitation dominates the E/P ratio, and therefore the water resource available through runoff. In summer, however, the evapotranspiration dominates over precipitation, which is a well-known characteristic of the Mediterranean region (e.g. Mariotti et al. 2002). Two of the limitations upon evapotranspiration are temperature and the availability of surface water. Given limitless water supply, the higher surface temperatures of the summer months should bring about greater evapotranspirative fluxes. In the Mediterranean region, evapotranspiration increases with rising temperatures through the spring and into summer, becoming the dominant term in the E/P ratio. Then, as summer progresses, evapotranspiration declines, first because of the limiting factor of reduced water availability from reduced rainfall during the same season, and second as the seasonal cycle of temperature takes a downward trajectory.

In a similar way, the controls on the *changes* in runoff in the future can be explored via the ratio between changes in evapotranspiration and changes in precipitation (ΔE/ΔP ratio). If the ratio is greater than one, it indicates that ΔE is the dominant term, and conversely if it is less than one, ΔP is dominant. The sign of the

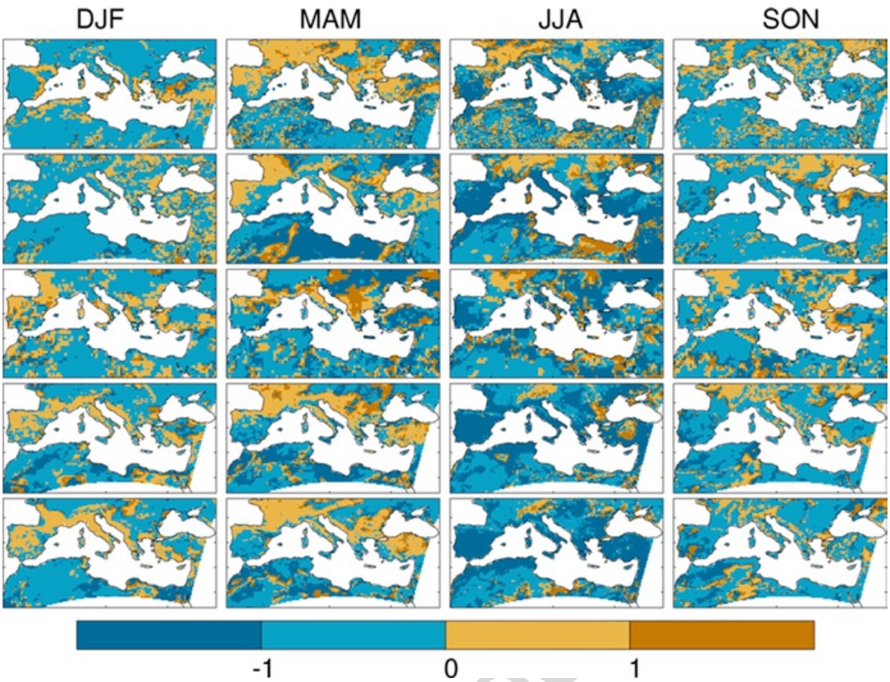


**Fig. 8.11** Seasonal ΔE/ΔP ratio in 2041–2050 relative to the 1961–1990 *baseline*. As before, row 1: ENEA; row 2: MPI; row 3: Météo-France; row 4: HadRM3-MOSES1; row 5: HadRM3-MOSES2. Values greater than |1| indicate that ΔE is the dominant term, and values less than |1| indicate that ΔP is the dominant term. Positive values show where ΔE and ΔP are working together in terms of their effect on runoff



ΔE/ΔP ratio demonstrates whether the two terms are acting together or against one another in terms of the effect on runoff. For example, if precipitation is decreasing while evapotranspiration is increasing, they both act to reduce runoff. Conversely, if evapotranspiration is also decreasing, it would oppose the change in precipitation with respect to the effect on runoff. For this part of the analysis, the sign of the evaporation term is multiplied by −1 such that the moisture flux has the same direction as precipitation. Therefore, a positive sign indicates that ΔE and ΔP are both acting in the same direction with respect to change in runoff. Figure 8.11 shows the ΔE/ΔP ratio for the 2041–2050 decade in relation to the 1961–1990 baseline. During much of the year, $\Delta E/\Delta P < |1|$, indicating that simultaneous changes in runoff are dominated by the changes in precipitation. In the summer season, however, the change in evapotranspiration is dominant across large parts of the Mediterranean domain, marked by a ratio of above one. The negative sign of the ratio across most of the region through much of the year demonstrates that the changes in precipitation are acting against changes in evapotranspiration in terms of their effect on runoff. This can be explained in part through the availability of water, as described above. When rainfall decreases, there is less water to evaporate, and vice versa.

However, particularly in the spring season, there are large areas of the northern Mediterranean region where the ΔE/ΔP ratio is positive. This highlights areas where rainfall is declining, but evapotranspiration is increasing owing to rising temperatures and sufficient available water. Changes in both terms act to reduce runoff, and so it is in spring that runoff is most highly sensitive to climate change.

Maps of change in precipitation–evapotranspiration (ΔP–ΔE) (Fig. 8.10c) demonstrate how runoff would be expected to change if just controlled by simultaneous changes in rainfall and evapotranspiration. Spring (March to May) stands out as being the season of the greatest reductions in ΔP–ΔE in the Mediterranean region across all of the models, changes which are largely reflected in the model runoff. Summer season (June to August) changes in model runoff are relatively small (Fig. 8.10d). Even though there are strong reductions in precipitation, reductions in evapotranspiration are as large or often larger. Soil moisture provides plants with transpirable water, and lower soil moisture brought by reductions in precipitation have nonlinear effects on the stomatal conductance and hence transpiration of the plants. The ΔP–ΔE term is positive across large areas of the Mediterranean, suggesting that runoff should increase. The fact that changes in model runoff does not change or decreases a little indicates that the water storage component (soil or canopy moisture) in the model plays a role in modifying runoff, and may allow for lags within the system. There are large differences between ΔP–ΔE and change in runoff at the seasonal time scale, but these are small at the annual time scale, which supports the possibility that time lags exist with the model system.

We can examine in greater detail how the seasonal cycle of rainfall and evapotranspiration compare between the models, and how they are projected to change in the future. Monthly mean precipitation and evapotranspiration for the baseline period and future decades were area-averaged across boxes of 10° longitude × 5° latitude (land areas only) across the Mediterranean region. South of the Mediterranean Sea, values of both P and E throughout the year are very small (<1 mm/day, except in coastal North Africa of the western part of the domain, where higher levels of rainfall permit greater evapotranspiration). Therefore a region to the north, where precipitation and evapotranspiration are larger, was selected to demonstrate how the seasonal cycle is projected to change through time (Fig. 8.12). The relatively large size of the region across which the P and E terms were averaged was intended to display broad-scale messages about the seasonal cycle and changes through time. On the other hand, it is likely that in places, the signal could be obscured through the influence of finer-scale variations in seasonal cycle characteristics and patterns of change. In the region displayed in Fig. 8.12, (approx. 10°E–20°E; 40°N–45°N) which covers much of Italy and the coastal region from Croatia to Albania, there was consistency between the models in the projected changes to the seasonal cycle.

It is immediately clear that the models do vary in the quantity and seasonal cycle of rainfall and evapotranspiration in this region, (particularly in the case of the Météo-France model (Fig. 8.12c), which shows a much less pronounced seasonal cycle in precipitation) but also that there are common features between the models. During winter, rainfall is relatively high, falling to a minimum in summer and rising

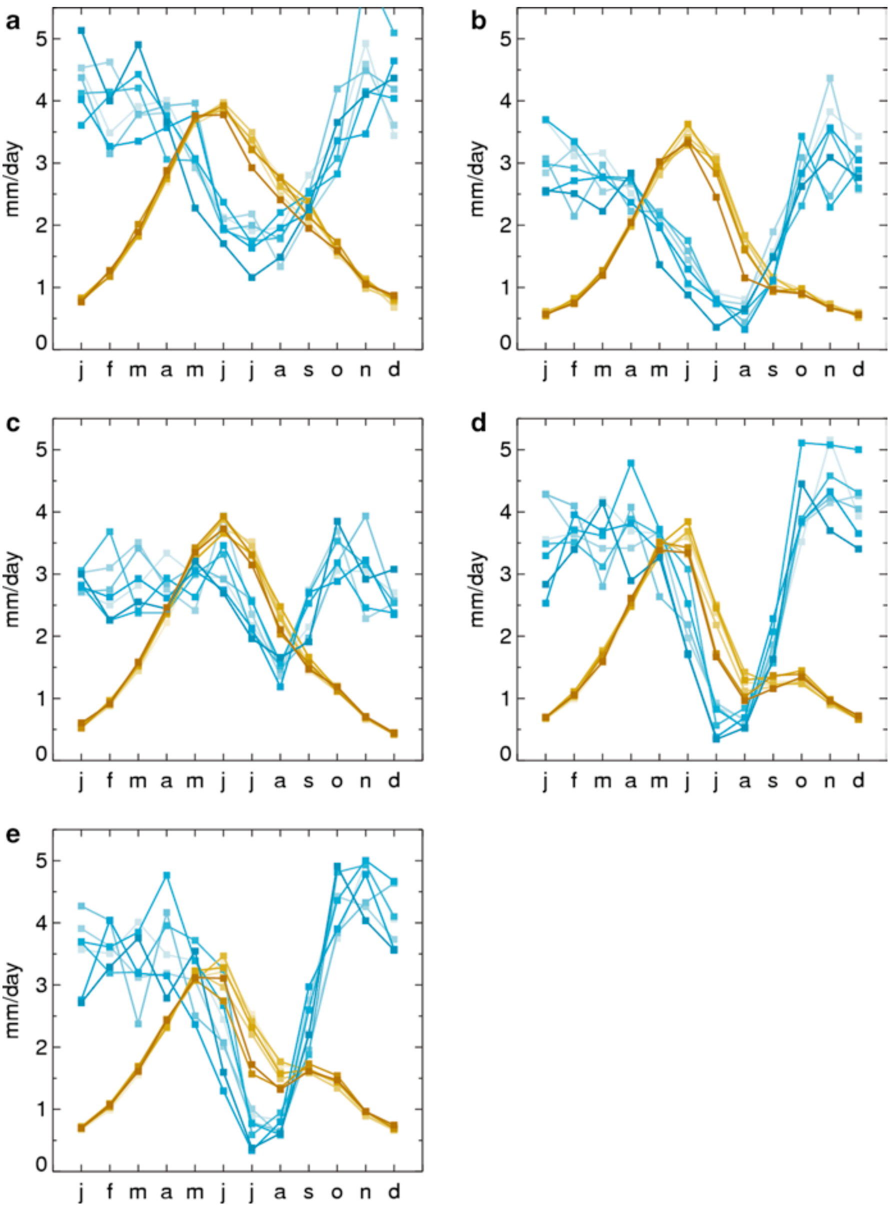


**Fig. 8.12** Monthly mean precipitation (*blue*) and evapotranspiration (*orange*) for the 30-year 1961–1990 baseline overlaid with decadal means from 1990s to 2040s. The *baseline* is marked in the palest *shade*, with the decadal means in progressively darker shades through time – 2040s precipitation is in the *darkest blue* and 2040s evaporation in the *darkest orange*. These are area-average means across a 10° longitude × 5° latitude box, approx. 10°E–20°E; 40°N–45°N. in each model: (**a**) ENEA; (**b**) MPI; (**c**) Météo-France; (**d**) HadRM3-MOSES1; (**e**) HadRM3-MOSES2

again through autumn. Evapotranspiration in each case follows a roughly opposite seasonal cycle. During winter, when temperatures are low, evapotranspiration is at a minimum, rising to a peak during June, before declining again. The minimum in rainfall occurs approximately a month or two after the maximum in evapotranspiration. Even though precipitation is declining during the spring season, the soil moisture store provides sufficient water such that it is not a limiting factor on evapotranspiration, which continues to increase as temperatures increase until June. In summer, as the soil dries out, the reduction in availability of transpirable water begins to limit the rate of evapotranspiration.

Figure 8.12 shows how the seasonal cycle changes for both variables, starting with the 1961–1990 thirty-year baseline in the palest shade, overlaid with decadal means in progressively darker shades to 2050. The decadal monthly mean rainfall has a noisy signature, affected by interannual variability, but the trend towards drier conditions in the summer months is discernable. The models tend to project a move towards dry conditions earlier in the year, again highlighting the spring transition months as sensitive to change. As water available from rainfall reduces, so too does the evapotranspiration, resulting in the progressive decline in summer quantities visible in each of the models in Fig. 8.12.

There is a recognized role for soil moisture in controlling rainfall via moisture made available through evapotranspiration. Anomalous drying of the soils during spring can inhibit evapotranspiration and hence moisture available for precipitation in the summer season. Positive feedbacks between soil moisture and precipitation anomalies can then develop in summer to enhance any initial drying (Kendon et al. 2009). While the analysis carried out in this multi-model study illustrates potential mechanisms for changes rather than diagnoses them, previous climate model experiments have been designed to partition the influence of different summer drying mechanisms in the Mediterranean region. Using a European RCM version of climate model HadAM3P, Rowell and Jones (2006) find that springtime soil moisture anomalies play an important role in changes in summer rainfall, while the summer soil moisture feedback is less so, but acts to enhance other drying effects. They also assess the reliability of the future decline in summer rainfall and note the importance of good representations of the physical process involved. Representing these soil moisture to rainfall mechanisms would rely on the models at their current resolution being able to simulate the full process: the transfer of moisture from the surface to the boundary layer, and from there to the formation of cloud and rain (Rowell and Jones 2006). In addition, there may be fine sensitivities or threshold behavior in the system connecting evapotranspiration with convective rainfall (Millán et al. 2005) that are poorly understood, or not represented within climate models. Further work could be done to determine the locations and temporal and spatial resolutions at which these would be important processes in comparison with other influences. Improvements in this area may be important not only in simulating mean rainfall and future trends, but also when considering rainfall characteristics such as intensity, location and timing. Future changes in variability and extremes in rainfall may have profound impacts upon a number of sectors including water resource management, even where mean changes are small (Kendon et al. 2009).

### *8.3.5 Summary*

Consistent with the global model projections, each of the five high-resolution models simulate higher temperatures and reduced evapotranspiration and precipitation for much of the Mediterranean region by the middle of this century. The strongest and most widespread reductions in precipitation projected to occur in the spring and summer seasons, while reductions in evapotranspiration are most severe in summer. As higher temperatures in all cases are projected for the 2040s, which should act to boost evapotranspiration, the decline is likely to be due to lack of available water.

Although there are discrepancies between the models in the patterns and magnitude of change, there are broad areas of consensus, including large summer reductions in both precipitation and evapotranspiration in the Iberian Peninsula, coastal southern France, Italy, southern and western Turkey, and parts of North Africa. From the perspective of renewable surface water resources (runoff), these negative anomalies in both evapotranspiration and precipitation have opposing effects, with the result that runoff anomalies in this season are relatively small. However, during spring (March to May), when seasonally increasing temperatures combined with sufficient surface water promote increased evapotranspiration, precipitation is beginning to decline earlier than in the baseline period. It is in the spring season that runoff appears to be most sensitive to climate change, particularly across the northern Mediterranean region, when the largest seasonal reductions are experienced in all models. These changes could have important implications for water dependent sectors in the region such as rain-fed and irrigated agriculture (Book Chapter on agriculture) and the natural vegetation, which could in turn feed back on the local climate system.

There remain many questions arising from this analysis, several of which are related to how the models simulate important processes affecting the water cycle across the Mediterranean. While there are some consistent messages in the model results, there exist differences as well, both in the baseline climatologies and the patterns and magnitude of changes. Even in places where there is broad agreement in the pattern of change, fine-scale differences can lead to very different projections for particular locations around the Mediterranean. What are the reasons behind model disagreement? Are they related to large-scale conditions or small-scale variations? For example, the control of soil moisture over evapotranspiration is a source of large uncertainty where relatively small biases in baseline soil moisture climatology can potentially translate to large changes in projections of future evapotranspiration. Of course, inter-model disagreement can point to deficiencies in our understanding of existing processes in the Mediterranean and hence our modeling of such processes, and it highlights the continued need for more observational studies.

Finally, there are questions related to how these results may be used to inform water resource management and adaptation decision-making, and if and how current practices would need to change in order to become sustainable.

## 8.4 Final Conclusions

The water cycle components over the Mediterranean both for current and future runs are studied with different global and high-resolution regional models yielding the primary following conclusions:

The projected mean annual change rate of precipitation (P) for the Mediterranean for the end of this century (21st) for both sea and land, are of about −10%. In pockets of Turkey, the eastern Mediterranean, Italy and Spain, projections from the high-resolution models are for even larger decreases in summer rainfall that reach 50% or more.

Projected changes for evaporation (E) are increasing over sea by the order of 7–9% and decreasing over land by about 4–8%. The net moisture budget, P-E, shows that the eastern Mediterranean will become even drier than the western Mediterranean. The river global and regional models all agree about significant decreases in future water inflow to the Mediterranean of as high as about 40% (excluding the Nile).

Furthermore, the Palmer Drought Severity Index (PDSI), which reflects the combined effects of precipitation and surface temperature changes, shows a progressive and substantial drying of Mediterranean land surface over this region since 1900 (−0.2 PDSI units/decade) consistent with a decrease in precipitation and an increase in surface temperatures.

Consistent with the global model projections, all the high-resolution models analyzed in this study simulate higher temperatures and reduced evapotranspiration and precipitation for much of the Mediterranean region by the middle of this century. However, the strongest and most widespread reductions in precipitation projected to occur in the spring and summer seasons, while reductions in evapotranspiration are most severe in summer.

**Acknowledgements** This study was supported by the EU-CIRCE and the GLOWA-JR projects. [AU5] Partial support was given by the Israel Water Authority. The model simulation was performed under the framework of the KAKUSHIN program funded by MEXT, Japan. Special thanks due to an anonymous reviewer for his/her valuable and constructive suggestions.



## References [AU6]

Adler RF et al (2003) The version 2 Global Precipitation Climatology Project (GPCP) monthly precipitation analysis (1979-present). J Hydrometeorol 4:1147–1167

Alpert P, Neeman BU, Shay-El Y (1990) Intermonthly variability of cyclone tracks in the Mediterranean. J Climate 3:1474–1478

Alpert P, Osetinsky I, Ziv B, Shafir H (2004) Semi-objective classification for daily synoptic systems: application to the Eastern Mediterranean climate change. Int J Climatol 24:1001–1011

Alpert P, Krichak SO, Osetinsky I, Dayan M, Haim D, Shafir H (2008) Climatic trends to extremes employing regional modeling and statistical interpretation over the E Mediterranean. Glob Planet Change 63:163–170

Arora VK, Boer GJ (1999) A variable velocity flow routing algorithm for GCMs. J Geophys Res 104(D24):30 965–30 979

Bethoux JP et al (1998) Warming and freshwater budget change in the Mediterranean since the 1940s, their possible relation to the greenhouse effect. Geophys Res Lett 25(7):1023–1026

Chou C, Neelin JD (2003) Mechanisms limiting the northward extent of the northern summer monsoons over North America, Asia, and Africa. J Climate 16:406–425

Cox PM, Betts RA, Bunton CB, Essery RLH, Rowntree PR, Smith J (1999) The impact of new land surface physics on the GCM simulation of climate and climate sensitivity. Clim Dyn 15:183–203

Diaz HF, Holerling MP, Eischeid JK (2001) ENSO variability, teleconnections and climate change. Int J Climatol 21:1845–1862

Fraedrich K (1994) ENSO impact on Europe?—a review. Tellus 46A:541–552

Gibelin AL, Deque M (2003) Anthropogenic climate change over the Mediterranean region simulated by a global variable resolution model. Clim Dyn 20:237–339

Giorgi F (2006) Climate change hot-spots. Geophys Res Lett 33(8):L08707

Giorgi F, Lionello P (2008) Climate change projections for the Mediterranean region. Glob Planet Change 63(2–3):90–104

Gordon C, Cooper C, Senior CA, Banks H, Gregory JM, Johns TC, Mitchell JFB, Wood RA (2000) The simulation of SST, sea ice extents and ocean heat transports in a version of the Hadley Centre coupled model without flux adjustments. Clim Dyn 16:147–168

Held IM, Soden BJ (2006) Robust responses of the hydrological cycle to global warming. J Climate 19:5686–5699

Hemming D, Buontempo C, Burke E, Collins M, Kaye N (2010) How uncertain are climate model projections of water availability indicators across the Middle East? Philos Trans R Soc A 368:5117–5135. doi:10.1098/rsta.2010.0174

Hurrell JW (1995) Decadal trends in the North-Atlantic Oscillation – regional temperatures and precipitation. Science 269(5224):676–679

IPCC (2007a) In: Solomon S, Qin D, Manning M, Chen Z, Marquis M, Averyt KB, Tignor M, Miller HL (eds) Climate change 2007: the physical science basis. Contribution of working group I to the fourth assessment report of the Intergovernmental Panel on Climate Change. Cambridge University Press, Cambridge/New York, 996 pp

IPCC (2007b) In: Parry ML, Canziani OF, Palutikof JP, van der Linden PJ, Hanson CE (eds) Contribution of working group II to the fourth assessment report of the Intergovernmental Panel on Climate Change, 2007. Cambridge University Press, Cambridge/New York, 976 pp

Jin FJ, Zangvil A (2009) Relationship between moisture budget components over the eastern Mediterranean. Int J Climatol. doi:10.1002/joc.1911

[AU7] Jin FJ, Kitoh A, Alpert P (2009) The atmospheric moisture budget over the Eastern Mediterranean based on a high-resolution global model – past and future. (Submitted)

Johanson CM, Fu Q (2009) Hadley cell widening: model simulations versus observations. J Climate 22:2713–2725

Josey S (2003) Changes in the heat and freshwater forcing of the eastern Mediterranean and their influence on deep water formation. J Geophys Res 108(C7):3237

Jung T et al (2006) Response to the summer of 2003 Mediterranean SST anomalies over Europe and Africa. J Climate 19(20):5439–5454

Kendon EJ, Rowell DP, Jones RJ (2009) Mechanisms and reliability of future projected changes in daily precipitation. Clim Dyn. doi:10.1007/s00382-009-0639-z

Kitoh A, Yatagai A, Alpert P (2008a) First super-high-resolution model projection that the ancient Fertile Crescent will disappear in this century. Hydrol Res Lett 2:1–4. doi:10.3178 HRL.2.1

Kitoh A, Yatagai A, Alpert P (2008b) Reply to comment by Ben-Zvi and Givati On first super-high-resolution model projection that the ancient Fertile Crescent will disappear in this century. Hydrol Res Lett 2:46

Krahmann G (1998) Longterm increases in Western Mediterranean salinities and temperatures: anthropogenic and climatic sources. Geophys Res Lett 25:4209–4212

Krichak SO, Alpert P, Dayan M (2004) The role of atmospheric processes associated with hurricane Olga in the December 2001 floods in Israel. J Hydrometeorol 5(6):1259–1270

Lozier MS, Stewart NM (2008) On the temporally varying northward penetration of Mediterranean overflow water and eastward penetration of Labrador Sea. J Phys Oceanogr 38:2097–2103

Lu J, Vecchi G, Reichler T (2007) Expansion of the Hadley cell under global warming. Geophys Res Lett 34:L06805. doi:10.1029/2006GL028443

Mariotti A (2009) Recent changes in Mediterranean water cycle: a pathway toward long-term regional hydroclimatic change? J Climate 23(6):1513–1525 [AU8]

Mariotti A (2010) Recent changes in Mediterranean water cycle: a pathway toward long-term regional hydroclimatic change? J Climate 23(1513–1525)

Mariotti A et al (2002) The hydrological cycle in the Mediterranean region and implications for the water budget of the Mediterranean Sea. J Climate 15(13):1674–1690

Mariotti A, Zeng N, Yoon JH, Artale V, Navarra A, Alpert P, Li ZX (2008) Mediterranean water cycle changes: transition to drier 21st century conditions in observations and CMIP3 simulations. Environ Res Lett 3:044001 (8 pp). doi:10.1088/1748-9326/3/4/044001

Millán MM, Estrela MJ, Sanz MJ, Mantilla E, Martín M, Pastor F, Salvador R, Vallejo R, Alonso L, Gangoiti G, Ilardia JL, Navazo M, Albizuri A, Artíñano B, Ciccioli P, Kallos G, Carvalho RA, Andrés D, Hoff A, Werhahn J, Seufert G, Versino B (2005) Climatic feedbacks and desertification: the Mediterranean model. J Climate 18:684–701

Millot C, Candela J, Fuda JL, Tber Y (2006) Large warming and salinification of the Mediterranean outflow due to changes in its composition. Deep-Sea Res I 53:656–666

Mizuta R, Oouchi K, Yoshimura H, Noda A, Katayama K, Yukimoto S, Hosaka M, Kusunoki S, Kawai H, Nakagawa M (2006) 20-km-mesh global climate simulations using JMA-GSM model Mean climate states. J Meteorol Soc Jpn 84:165–185

Mizuta R, Adachi Y, Yukimoto S, Kusunoki S (2008) Estimation of the future distribution of sea surface temperature and sea ice using the CMIP3 multi-model ensemble mean, Technical report of the Meteorological Research Institute, no.56. Meteorological Research Institute, Tokyo, 28 pp [AU9]

Oki T, Sud YC (1998) Design of Total Runoff Integrating Pathways (TRIP)—A global river channel network. Earth Interact 2. Available online at http://EarthInteractions.org

Oki T, Nishimura T, Dirmeyer P (1999) Assessment of annual runoff from land surface models using Total Runoff Integrating Pathways (TRIP). J Meteorol Soc Jpn 77:235–255

Pal JS et al (2004) Consistency of recent European summer precipitation trends and extremes with future regional climate projections. Geophys Res Lett 31:L13202 [AU10]

Potter RA, Lozier MS (2004) On the warming and salinification of the Mediterranean outflow waters. Geophys Res Lett 31:L01202

Price C, Stone L, Huppert A, Rajagopalan B, Alpert P (1998) A possible link between El Niño and precipitation in Israel. Geophys Res Lett 25:3963–3966

Reddaway JM, Bigg GR (1996) Climate change over the Mediterranean and links to the more general atmospheric circulation. Int J Climatol 16:651–661

Reid JL (1979) On the contribution of the Mediterranean Sea outflow to the Norwegian-Greenland Sea. Deep Sea Res Part A 26:1199–1223

Rixen M et al (2005) The Western Mediterranean deep water: a proxy for climate change. Geophys Res Lett 32(12):L12608

Rodwell MJ, Hoskins BJ (1996) Monsoons and the dynamic of deserts. Q J R Meteorol Soc 122:1385–1404

Roether W et al (2007) Transient Eastern Mediterranean deep waters in response to the massive dense-water output of the Aegean Sea in the 1990s. Prog Ocean 74:540–571

Rohling EJ, Bryden HL (1992) Man-induced salinity and temperature increase in Western Mediterranean deep water. J Geophys Res 97:11191–11198

Rohling EJ, Hilgen FJ (1991) The eastern Mediterranean climate at times of sapropel formation: a review. Geologie en Mijnbouw 70:253–264

Rowell DP, Jones RJ (2006) Causes and uncertainty of future summer drying over Europe. Clim Dyn 27:281–299

Sanchez-Gomez E et al (2009) Future changes in the Mediterranean water budget projected by an ensemble of Regional Climate Models. Geophys Res Lett 36(21):L21401

Seager R, Ting MF, Held I, Kushnir Y, Lu J, Vecchi G, Huang HP, Harnik N, Leetmaa A, Lau NC, Li CH, Velez (Miller) J, Naik N (2007) Model projections of an imminent transition to a more arid climate in southwestern North America. Science 316(5828):1181–1184

Sheffield J, Wood EF (2008) Projected changes in drought occurrence under future global warming from multi-model, multi scenario, IPCC AR4 simulations. Clim Dyn 31(1):79–105

Skliris N et al (2007) Hydrological changes in the Mediterranean Sea in relation to changes in the freshwater budget: a numerical modelling study. J Marine Syst 65(1–4):400–416

Tsimplis MN et al (2008) 21st century Mediterranean sea level rise: steric and atmospheric pressure contributions from a regional model. Glob Planet Change 63(2–3):105–111

[AU11] Ulbrich U et al (2006) The Mediterranean climate change under global warming. In: Lionello P (ed) Mediterranean climate variability and predictability. Elsevier, Burlington, pp 398–415

Wentz FJ et al (2007) How much more rain will global warming bring? Science 317(5835):233–235

Yu LS (2007) Global variations in oceanic evaporation (1958–2005): the role of the changing wind speed. J Climate 20:5376–5390

Yu LS, Weller RA (2007) Objectively analyzed air-sea heat fluxes for the global ice-free oceans (1981–2005). Bull A Meteorol Soc 88(4):527–539

Ziv B, Saaroni H, Alpert P (2004) The factors governing the summer regime of the Eastern Mediterranean. Int J Climatol 24:1859–1871

Ziv B, Saaroni H, Baharad A, Yekutieli D, Alpert P (2005) Indications for aggravation in summer heat conditions over the Mediterranean basin. Geophys Res Lett 32:L12706. doi:10.1029/2005GL022796

# Author Queries

Chapter No.: 8 0001771868

| Queries | Details Required | Author's Response |
|---|---|---|
| AU1 | Please provide Department name of authors "Alpert, Hemmings, Jin, Kay, Kitoh" in affiliation. | |
| AU2 | Please confirm the alignment of Table 8.1 and 8.3 is appropriate. | |
| AU3 | All occurrences of "E-P" have been changed to "E–P". Please confirm the change is appropriate. | |
| AU4 | Essery et al. (2003) is cited in text but not given in the reference list. Please provide details in the list or delete the citation from the text. | |
| AU5 | Please confirm the placement of "Acknowledgement" is appropriate. | |
| AU6 | Please provide in-text citation for deference Mariotti (2009). | |
| AU7 | Please update the reference Jin et al. (2009). | |
| AU8 | Please confirm the updated reference Mariotti (2009). | |
| AU9 | Please confirm the inserted details for the reference Mizuta et al. (2008). | |
| AU10 | Please confirm the inserted page range for the reference Pal et al. (2004). | |
| AU11 | Please confirm the inserted publisher location for the reference Ulbrich et al. (2006). | |